Ecological Modelling 472 (2022) 110097

Contents lists available at ScienceDirect

Ecological Modelling

journal homepage: www.elsevier.com/locate/ecolmodel

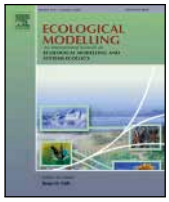

# Understanding the drivers of fish variability in an end-to-end model of the Northern Humboldt Current System

Mariana Hill Cruz [a,*], Ivy Frenger [a], Julia Getzlaff [a], Iris Kriest [a], Tianfei Xue [a], Yunne-Jai Shin [b]

[a] GEOMAR Helmholtz Centre for Ocean Research Kiel, Duesternbrooker Weg 20, 24105, Kiel, Germany
[b] IRD (Institut de Recherche pour le Developpement) – UMR 248 MARBEC (IRD-IFREMER-CNRS-Universite Montpellier), av Jean Monnet CS 30171, 34203 Sete cedex, France

ARTICLE INFO

*Keywords:*
Ecosystem modelling
OSMOSE
End-to-end model
CROCO
BioEBUS
Northern Humboldt Current System
Eastern boundary upwelling system
Fisheries
Higher trophic levels
Trophic interactions
physical–biogeochemical model

ABSTRACT

The Northern Humboldt Current System is the most productive eastern boundary upwelling system, generating about 10 % of the global fish production, mainly coming from small pelagic fish. It is bottom-up and top-down affected by environmental and anthropogenic variability, such as El-Niño Southern Oscillation and fishing pressure, respectively. The high variability of small pelagic fish in this system, as well as their economic importance, call for a careful management aided by the use of end-to-end models. This type of models represent the ecosystem as a whole, from the physics, through plankton up to fish dynamics. In this study, we utilised an end-to-end model consisting of a physical–biogeochemical model (CROCO-BioEBUS) coupled one-way with an individual-based fish model (OSMOSE). We investigated how time-variability in plankton food production affects fish populations in OSMOSE and contrasted it against the sensitivity of the model to two parameters with high uncertainty: the plankton accessibility to fish and fish larval mortality. Relative interannual variability in the modelled fish is similar to plankton variability. It is, however, small compared with the high variability seen in fish observations in this productive ecosystem. In contrast, changes in larval mortality have a strong effect on anchovies. In OSMOSE, it is a common practice to scale plankton food for fish, accounting for processes that may make part of the total plankton in the water column unavailable. We suggest that this scaling should be done constant across all plankton groups when previous knowledge on the different availabilities is lacking. In addition, end-to-end modelling systems should consider environmental impacts on other biological processes such as larval mortality in order to better capture the interactions between environmental processes, plankton and fish.

## 1. Introduction

The Northern Humboldt Current System (NHCS), located in the eastern-tropical south Pacific (ETSP) ocean, is the most productive eastern boundary upwelling system, generating about up to 10% of the global fish production (Chavez et al., 2008; FAO, 2020). It hosts the largest single-species fishery of the planet, the Peruvian anchovy (*Engraulis ringens*) (Chavez et al., 2003; Aranda, 2009). Along with the Pacific sardine (*Sardinops sagax*), these small pelagic fish feed on plankton and build up huge biomasses that support a large industry of fishmeal production. They are also valued by the local communities culturally (López de la Lama et al., 2021) and economically (Christensen et al., 2014), and are consumed by many marine predators such as seabirds (Muck, 1987; Jahncke et al., 2004), marine mammals (Majluf and Reyes, 1989) and larger predatory fish (Pauly et al., 1987). However, they have shown to be prone to collapses related to environmental variability along with overfishing (Boerema and Gulland, 1973), putting at risk the fishing industry (Paredes and Gutierrez, 2008). The drivers behind the disproportionately large fish production of the NHCS compared to other eastern boundary upwelling systems are not fully understood (Carr, 2002). Possible explanations include the reset of the system succession to small pelagic fish during the El-Niño periods (Bakun and Broad, 2003), the compression of zooplankton prey for small pelagic fish at the surface by a shallow oxygen minimum zone, and increased trophic transfer efficiency caused by relatively weak winds in combination to high primary production (Chavez and Messié, 2009).

The ETSP is affected by strong interannual variability. In addition to the El-Niño and La-Niña events, the ETSP is subjected to regimes of cold ocean temperature, named La Vieja, and warm temperature, called El Viejo (Chavez et al., 2003). Anchovies and sardines also fluctuate interannually with regimes of high anchovy abundance alternating with regimes of high sardine abundance (Schwartzlose et al., 1999; Chavez et al., 2003). Causes for these fluctuations are not completely

* Corresponding author.
*E-mail address:* mhill-cruz@geomar.de (M. Hill Cruz).

https://doi.org/10.1016/j.ecolmodel.2022.110097
Received 9 February 2022; Received in revised form 12 July 2022; Accepted 3 August 2022
Available online 29 August 2022

clear and have been related to interannual variability in water temperature (Chavez et al., 2003). Between the 1970s and 1990s, the ecosystem was under a regime of abundant sardines. The regime shifted during the 1990s towards an anchovy-dominated ecosystem. Anchovy collapsed during the El-Niño of 1998 but managed to recover while sardines continued declining to almost no presence by 2000 (Chavez et al., 2003; Alheit and Niquen, 2004). In addition, red squat lobsters (*Pleuroncodes monodon*), a generally benthic species off central Chile but mostly pelagic off Peru (Gutiérrez et al., 2008), became particularly abundant in the pelagic system after this event (Gutiérrez et al., 2008). Finally, the system is both bottom-up and top-down affected by environmental and anthropogenic drivers, such as changes in temperature and productivity due to El-Niño Southern Oscillation, and fishing pressure, respectively (Boerema and Gulland, 1973; Barrett et al., 1985; Barber and Chavez, 1983). The high and poorly understood temporal variability of fishes in the NHCS, as well as their importance for the economy, food security and the rest of the ecosystem, call for a careful and sustainable fisheries management using an ecosystem-based-management approach supported by end-to-end models (Pikitch et al., 2004).

End-to-end models aim at representing the marine ecosystems as a whole by including environmental components as well as lower (plankton) and higher trophic levels (HTL) such as fish and their utilisation by humans. Common ecosystem models represent functional groups or individual species interacting in a trophic web (see Fulton, 2010; Tittensor et al., 2018, for reviews). End-to-end models also include primary producers, such as plankton, which are affected by the environment, either already included in the model (e.g., Atlantis; Fulton et al., 2004) or provided by physical–biogeochemical models (e.g., PISCES-APECOSM; Maury, 2010). Among other types of ecosystem models, the multispecies individual-based models are as detailed as simulating the single individuals or schools of fish (e.g., Rose et al., 2015). Belonging to such type of models, the Object-oriented Simulator of Marine Ecosystems (OSMOSE) simulates the whole life cycle of fish (Shin and Cury, 2001, 2004, www.osmose-model.org [Accessed: 2021-10-28]). It is usually one-way coupled with biogeochemical models which provide lower trophic levels, or plankton, as food for some of the fish in the ecosystem (e.g., Halouani et al., 2016; Moullec et al., 2019b). In this study, we simulated the ETSP ecosystem with a one-way coupled model system including a physical–biogeochemical model (Coastal and Regional Ocean COmmunity model (CROCO) - Biogeochemical model developed for the Eastern Boundary Upwelling Systems (BioEBUS); Shchepetkin and McWilliams, 2005; Gutknecht et al., 2013) and OSMOSE as HTL model.

To improve the model fit to observations, models have to be calibrated by adjusting model parameters for which no values are available easily or unambiguously from literature. Using optimisation algorithms – here in particular evolutionary algorithms – provides an automated and objective way for calibration, and can converge to solutions that may not be reached manually or analytically when handling complex models (Duboz et al., 2010; Oliveros-Ramos and Shin, 2016). Yet, the strong variability in physical forcing and in fish abundance observed in the NHCS makes the calibration of OSMOSE for this specific ecosystem challenging. OSMOSE has been implemented in several ecosystems using time-constant parameters to represent a steady ecosystem state (Travers et al., 2006; Fu et al., 2012; Grüss et al., 2015; Halouani et al., 2016; Xing et al., 2017; Bănaru et al., 2019; Moullec et al., 2019b), which can serve as a starting point for evaluating the ecosystem response under changing conditions (e.g., Fu et al., 2012; Moullec et al., 2019a; Diaz et al., 2019; Travers-Trolet et al., 2014b). Marzloff et al. (2009) developed a configuration of OSMOSE with time-constant parameters for the pelagic ecosystem off Peru using years 2000 to 2006 as reference for the calibration, just after the regime shift of 1998. On the other hand, Oliveros-Ramos et al. (2017) addressed the interannual variability of the NHCS by calibrating time-varying parameters. The resulting configuration matched the seasonal and interannual fluctuations in observations. This approach implicitly assumes that the observed variability in fish may be caused by processes that need to be accounted for by temporally varying parameter values and it provides an estimation for such parameters. However, it might dampen any variability caused bottom-up by fluctuations in physical forcing and its propagation to plankton biomass. On the other hand, using constant parameters allows to isolate the impact of time-variability in the forcings.

The aim of this study is to understand the sensitivity of OSMOSE to temporal variability in plankton food estimated by a physical–biogeochemical model, and whether this replicates the temporal variability that has historically been observed in fish. To do so, we first calibrated OSMOSE against biomass and landings data of nine fish and invertebrate species from the post-El-Niño, low-sardine regime between 2000 and 2008, period in which no strong El-Niño event occurred. To investigate the potential relevance of bottom-up causes of fluctuations of fish biomass, we decided here to apply a configuration of OSMOSE for the ETSP with calibrated temporally constant parameters. Such a set-up allows to systematically probe the ecosystem regarding its response to variability of food. For calibration, OSMOSE was forced with a plankton climatology that we obtained from the biogeochemical model (CROCO-BioEBUS) hindcast over the time-period from 2000 to 2008. We then forced the calibrated OSMOSE configuration with an interannually varying biogeochemical hindcast from 1990 to 2010 to assess whether or not the plankton forcing alone could generate the regime shift after the El-Niño of 1998 in OSMOSE. To put the effects of interannual forcing into perspective, we also carried out sensitivity experiments varying two different parameters of the OSMOSE model, which are either directly related to the food availability of the biogeochemical model, or address the larval mortality of fish species. These parameters have high uncertainty and, in previous studies, have often been adjusted to calibrate OSMOSE. We also evaluated both CROCO-BioEBUS and OSMOSE since this is a pre-condition for performing the experiments. The results of this study provide insight on advisable improvements for the connection of OSMOSE with biogeochemical models for a better representation of the effect of environmental variability in end-to-end models.

## 2. Methods

### 2.1. The lower trophic levels model: CROCO-BioEBUS

We used the Coastal and Regional Ocean COmmunity model (CROCO, Shchepetkin and McWilliams, 2005) coupled online with a Biogeochemical model developed for Eastern Boundary Upwelling Systems (BioEBUS, Gutknecht et al., 2013). The model domain spans from 10°N to 33°S and from 69° to 118°W with a horizontal resolution of $\frac{1}{12}°$ and 32 sigma layers. BioEBUS consists of 12 prognostic variables: oxygen, ammonium, nitrate, nitrite, nitrous oxide, dissolved organic nitrogen, small and large detritus, small and large phytoplankton, and small and large zooplankton. Initial and boundary conditions for CROCO-BioEBUS are from Simple Ocean Data Assimilation (SODA, Carton et al., 2018) and monthly climatology CARS (CSIRO-Commonwealth scientific and industrial research organisation Atlas of Regional Seas) observations (Ridgway et al., 2002). CROCO-BioEBUS is spun-up for 30 years repeating the forcing of year 1990. Afterwards, it is simulated from 1990 to 2010 with interannually-varying forcing. The configuration used in this study is described in detail by José et al. (2019) and a list of the parameters that were adjusted for this configuration is available in Xue et al. (2022).

For coupling with OSMOSE, the four plankton groups – small and large phyto- and zooplankton – were integrated above the oxygen minimum zone (OMZ; here defined by an oxygen threshold of 90 μmol $O_2$ $kg^{-1}$, Karstensen et al., 2008) and integrated biomasses were transformed from nitrogen to wet weight (WW, main currency in OSMOSE) by multiplying them by the conversion factors: 720, 720, 675 and

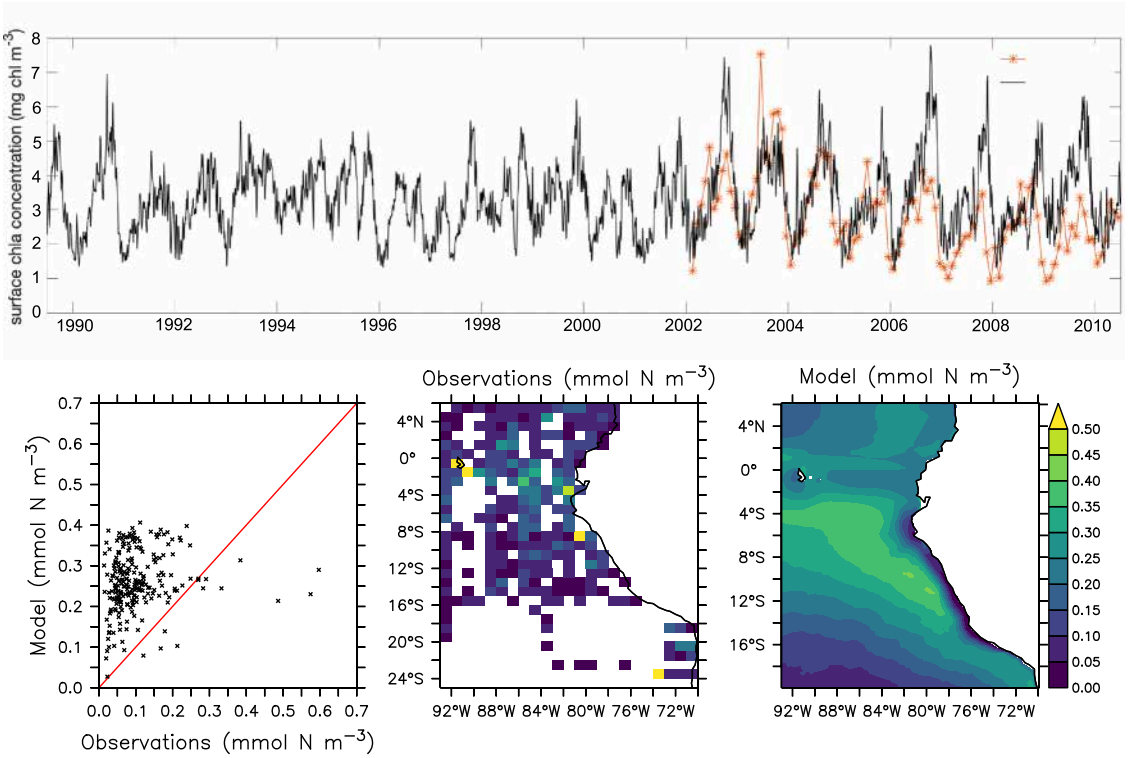


**Fig. 1.** Top: Surface chlorophyll concentration in the model (black) and in MODIS observations (red; NASA, 2018), averaged over the closest 2° off the coast of Peru from 15 to 5°S. Bottom: comparison of mesozooplankton observations from the global dataset by O'Brien and Moriarty (2012), Moriarty and O'Brien (2013) and simulated large zooplankton averaged over the upper 100 m depth (mmol N m$^{-3}$).

1000 mg WW mmol N$^{-1}$, respectively (Travers-Trolet et al., 2014a, their Tab. 4), regridded from $\frac{1}{12}$° to $\frac{1}{6}$° resolution, and then provided as food forcing for the fish in OSMOSE (see Section 2.2). Since CROCO-BioEBUS provides daily plankton food output, we averaged the plankton food to produce bi-weekly forcing for OSMOSE.

### 2.2. The higher trophic levels model: OSMOSE

OSMOSE is an object-oriented individual-based model that simulates the whole-life cycle of fish, from eggs to adults. Individual fish are grouped in schools of the same size and age. These are distributed over a 2-dimensional grid and within species and life stage specific distribution maps that are produced by statistical climate niche models (Oliveros-Ramos et al., 2017). On every time step, each school moves randomly to one adjacent grid cell within its distribution map. Predation is opportunistic, based on the spatial overlap of predator and prey. Every species or group feeds on prey that falls within certain minimum and maximum predator–prey size ratios. The predator feeds until either being satiated or until the available prey runs out. Satiation depends on the biomass of the predator, the number of mortality sub-steps and a constant maximum ingestion rate which, in our configuration, is the same for all groups (see Appendix A.2). In consequence, predatory interactions are not set *a priori* by the model user but these emerge from the size structure of the populations. A full description of the model is available in Shin and Cury (2001, 2004) and Travers et al. (2009).

#### 2.2.1. Configuration overview

The configuration in this project uses OSMOSE version 3.3.3 and was derived from the configuration by Oliveros-Ramos et al. (2017), which covers the same region, from 20°S to 6°N and from 93° to 70°W (see Fig. 1 bottom), spans from 1992 to 2008 and was calibrated against interannually-varying observations. For our configuration, we averaged the observations from 2000 to 2008, to produce a configuration representative of this period of time, after the strong El-Niño of 1998. Observations were available for all groups simulated in the model for this period of time. We also averaged the plankton simulated by CROCO-BioEBUS from 2000 to 2008 to produce a plankton climatology as forcing for OSMOSE. This time period is dominated by anchovies while sardines were dominant through the 1980s and decreased during the 1990s until their final collapse after the El-Niño event of 1997–1998 (Chavez et al., 2003). Although for the period that we used to calibrate the model (2000 to 2008) sardines play a minor role, they are an important component of the ecosystem in the long term so we included them in the configuration. We set up a configuration with constant parameters to generate a mechanistic model that can be used to understand the ecosystem response to certain forcings, such as fishing pressure and environmental changes, in sensitivity studies.

The configuration for the Northern Humboldt Current System (NHCS) consists of Peruvian anchovy (*Engraulis ringens*), Peruvian hake (*Merluccius gayi*), Pacific sardine (*Sardinops sagax*), Chilean jack mackerel (*Trachurus murphyi*), Pacific chub mackerel (*Scomber japonicus*), mesopelagic fish, squat lobster (*Pleurocondes monodon*), Humboldt squid (*Dosidicus gigas*) and euphausiids. Parameters as well as distribution maps for all groups are provided in Appendix A.2 and in the supplement. The parameters in our configuration are the same as in Oliveros-Ramos et al. (2017), with the exceptions mentioned in Section 2.2.2. We applied constant annual fishing rates for each species in our climatological set-up. Because anchovies are only fished during certain seasons, their landings show a marked seasonality. Therefore, a seasonality of fishing rate was derived from the anchovy landings observations (see Fig. 7 in the Appendix A.2). The fishing rate of all other species was assumed to be constant over the year. The model is initialised through a seeding process that generates schools of fish at the egg and larval stages during several years at the beginning of the model run. After the first 12 years of the spin-up, the seeding is stopped and all further eggs are only produced by adult fish. Therefore, egg production depends on the amount of adults biomass.

In OSMOSE, the spatial distribution of fish is constrained by maps defining their habitat. The maps define the probability of a school to occur on each of the grid cells of the domain, with the sum of all wet grid cells equalling 1. In our study, the distribution maps of each species vary for every season. At the beginning of the season, the schools are randomly located over the new map taking into account the probability given by each grid cell. We averaged the distribution maps of the configuration mentioned above, provided by Oliveros-Ramos and Lujan-Paredes (personal communication), from 2000 to 2008, to produce a seasonal climatology.

As part of the analysis performed in Section 3.3, we isolated the region where most of anchovies occur. To do so, we utilised a probability map calculated by averaging all temporally-varying maps. Based on this map, first, we excluded all cells with a chance of anchovy occurrence equal to 0, as well as the dry cells. Out of the remaining cells, we calculated the mean and then selected those cells with higher probability than the mean. There is a probability of around 90% of finding any of the anchovy schools within the region consisting of all selected cells.

#### 2.2.2. Model calibration

The model was calibrated using the evolutionary algorithm developed by Oliveros-Ramos et al. (2017). Detailed instructions on the calibration are available in the OSMOSE documentation: http://documentation.osmose-model.org/index.html. The calibration ran for 400 hundred generations using a population size of 75 individuals (an individual is a vector of parameter values in this calibration framework) per generation for the evolutionary algorithm. In every iteration, the model was run for 50 years consisting of 25 years of spin-up and evaluating against observations the last 25 years of the simulation. Available observations included biomasses from acoustic surveys integrated over the exclusive economic zone of Peru (EEZ) and averaged from 2000 to 2008, and monthly landings of exploited species (anchovy, hake, sardine, jack mackerel, chub mackerel and Humboldt squid) also averaged from 2000 to 2008. Because the acoustic indices only cover the EEZ of Peru, we scaled the model output by dividing it by a factor $q$ (see Table 4), which represents the proportion of the averaged distribution map of each group that falls within the Peruvian EEZ.

In their configuration, Oliveros-Ramos et al. (2017) calibrated a time-varying larval mortality (LM), constant natural additional mortality, time- and size-class-varying fishing rate, time-varying plankton accessibility coefficient (AC) and time-varying incoming flux of squat lobster. In our climatology, no incoming flux of squat lobster is included, because the squat lobster is present since the beginning of the simulation, and we only calibrated time-constant LM and plankton AC. Time-constant natural additional mortalities and fishing rates (with a seasonality for anchovies, see Section 2.2.1) were obtained from the literature (see Table 4). In addition, we manually adjusted the fishing rate of Humboldt squid before the calibration process since our configuration had a tendency to overestimate the landings of this species.

The AC is the fraction of the total plankton that is provided as food for the fish. It parameterises a range of processes that affect the availability of plankton for the fish such as turbulence, stratification and vertical migrations and distribution (see Travers-Trolet et al., 2014a). Literature values of this parameter for OSMOSE vary strongly, from very low values of $10^{-5}$% (Marzloff et al., 2009) up to 69% (Grüss et al., 2015). Our calibration suggested optimal values AC of 3.0, 5.0, 2.0 and 0.4% for small and large phytoplankton and zooplankton, respectively. The larval mortality rate (LM; $ts^{-1}$) is applied to the first stage of fish in OSMOSE (eggs and larvae) during its first time step (ts) of life. This parameter is typically calibrated for OSMOSE (e.g., Travers et al., 2009; Marzloff et al., 2009; Halouani et al., 2016; Bănaru et al., 2019) since field observations are scarce. The optimal parameter values are available in Table 4 in Appendix A.2.

After calibrating the model, we simulated the configuration for 300 years to evaluate its stability. With the calibrated parameters, the sardine population collapses after the initial 50 years of simulation (see Supplement). To avoid this decrease, we adjusted by hand the natural mortality of juvenile and adult sardine, as well as its LM (see Table 4 in Appendix A.2).

### 2.3. Model evaluation

We evaluated CROCO-BioEBUS by comparing chlorophyll concentration and large zooplankton against observations (see Section 3.1.1). Simulated phytoplankton concentration was converted to chlorophyll using function get_chla.m of the croco_tools package (Penven, 2019) and compared against MODIS remotely sensed chlorophyll concentration (NASA, 2018).

A previous version of the model (José et al., 2017) strongly overestimated zooplankton in comparison to observations (Hill Cruz et al., 2021). Therefore, for the present study, we tuned the model to better match observed concentrations. After tuning the model, large zooplankton model concentrations were compared against mesozooplankton observations by Moriarty and O'Brien (2013) and O'Brien and Moriarty (2012), which are provided in carbon units. For model comparison we transformed the observations to nitrogen dividing by a carbon to nitrogen ratio of 4.9 gC/gN (Kiørboe, 2013) and by the nitrogen molar mass of 14 g/mol. Because the model does not parameterise diel vertical migrations, simulated zooplankton is only present where food is available, within the upper 100 m. We therefore compared only the averaged zooplankton in the model and observations over the upper 100 m of the water column.

Further model evaluations of sea surface temperature and mixed layer depth are provided in Appendix A.1. Simulated oxygen evaluation is available in José et al. (2019).

We also evaluated the performance of OSMOSE by comparing trophic levels with literature values (Section 3.1.2).

### 2.4. Experimental design

To evaluate the effect and relative importance of an interannual versus a climatological plankton forcing on the simulated biomass of fish and macroinvertebrates, we carried out six simulations. All simulations ran for 25 years of spin-up followed by 21 years of simulation. Our starting point was the calibrated climatological set-up described in Section 2.2.2 (experiment 1 "climatological"). In this experiment, the 46 years run (25 years of spin-up and then 21 simulation years) have the same climatological plankton forcing. With the second and third experiments, we explored how interannually varying plankton affects the fish. Both experiments have an interannual plankton hindcast from 1990 to 2010 as forcing for the 21 years of simulation. The spin-up, however, differs in the two experiments to test whether variability in the spin-up approach has any impact on the sensitivity of fish to plankton forcing. For the second experiment, called "interannual", the spin-up consists of four years with climatological plankton forcing and then 21 years of interannual forcing. The third experiment ("hybrid") has climatological forcing over the entire 25 years of spin-up.

We also put the impact of interannual plankton forcing into perspective by comparing it against the effect of changing two parameters. We modified the plankton accessibility coefficient (AC) and the larval mortality (LM) by 10%. These parameters were calibrated in the original climatological set-up to optimise the model, and their uncertainty is high. In experiment 4 ("hybrid-AC"), we evaluated the effect of a reduction in the AC by 10% which translates into less plankton being available as potential food. In reality, this can be interpreted as, for example, zooplankton hiding in a shallower oxygen minimum zone, or a deeper mixed layer that dilutes phytoplankton. In our original climatological OSMOSE configuration, we calibrated a different AC for each of the four plankton groups. This adds an additional source of

variability by changing the relative contribution of each group to the diet of fish. We removed this variability in experiment 5 ("hybrid-eqAC") by setting the AC to a constant value of 10% for all plankton groups. We note that this represents a strong increase in the AC which makes the resulting fish biomass of this experiment not directly comparable to the other scenarios. Therefore, for this specific experiment, we only analysed the relative fluctuations in biomass. With all of the above experiments, we investigated the effect of changing food, i.e. the gains of fish biomass, either through the forcing, or through the AC. In a final sixth experiment ("Hybrid-aLM"), we investigated how these changes in the "gain", or food, side compare to changes in loss terms of fish, by increasing the LM of anchovies by 10%. We only manipulated the LM of anchovy in order to avoid an effect obscured by trophic interactions when manipulating the LMs of the other groups. To make the Hybrid-aLM and Hybrid-AC experiments comparable, we increased the LM and decreased the AC so that both experiments would have a negative impact on the anchovy biomass.

The six experiments are summarised below:

1. Climatological: 25 years spin-up with climatological plankton followed by 21 years of simulation using the same plankton climatology.
2. Interannual: The spin-up consisted of 4 years with climatological plankton forcing and then 21 years with interannual forcing. After the spin-up, we simulated an additional 21 years applying the interannual hindcast of plankton from 1990 to 2010.
3. Hybrid: 25 years of spin-up time with climatological plankton followed by 21 years of simulation using the interannual hindcast of plankton from 1990 to 2010.
4. Hybrid-AC: Hybrid set-up with AC reduced by 10%.
5. Hybrid-eqAC: Hybrid set-up with AC of all four plankton groups equal to 10%.
6. Hybrid-aLM: Hybrid set-up with anchovy LM increased by 10%.

Because OSMOSE is a stochastic model (random movement of schools and ordering of mortality events in a time-step), the output varies slightly among simulations. Therefore, we analysed the average of 20 model runs for each experiment.

This study explores the effect of plankton variability on OSMOSE. Therefore, we removed other sources of interannual variability, for instance habitat, by keeping climatological distribution maps in all configurations. Appendix A.5 provides the results of an alternative set-up where interannually-varying distribution maps were applied from 1992 to 2008 in the hybrid configuration.

## 3. Results

### 3.1. Model evaluation

#### 3.1.1. CROCO-BioEBUS

The model reproduces the temporal variability in chlorophyll observations generally well, replicating the seasonal pattern with higher chlorophyll concentrations in austral summer (Fig. 1 top). However, from 2006 on-wards it tends to overestimate chlorophyll, especially during the austral summer.

Large zooplankton is generally of the same order of magnitude as mesozooplankton observations (Fig. 1 bottom). This is a considerable improvement compared to the older version of the model by José et al. (2017) which was evaluated by Hill Cruz et al. (2021). Both, model and observations, show a high concentration of mesozooplankton in the region near the Equator as well as towards the coast of Peru. Within 50 km from the coast, large zooplankton declines in the model. This is not evident in the observations; however, this might be due to the low spatial resolution of observational samples. Further, observations show a hotspot of high mesozooplankton concentrations around the Galapagos Islands which is not visible in the model. This could be either a weakness of the model or it could also be an artefact in the observations due to averaging over very few samples for the whole water column. An extensive discussion on the possible causes of mismatch between simulated large zooplankton and mesozooplankton observations observed in an earlier version of BioEBUS is provided by Hill Cruz et al. (2021).

**Table 1**
Trophic levels reported in the literature in Ecopath models of the NHCS (1a, 1b and 2) and observations (3).
*Sources:* 1a, b Tam et al. (2008). 1a refers to a model of the ecosystem state between 1995–1996, during La-Niña conditions and 1b between 1997–1998 during El-Niño conditions. 2 Guénette et al. (2008). 3 Pizarro et al. (2019).

| | (1a) | (1b) | (2) | (3) |
|---|---|---|---|---|
| Anchovy | 2.35 | 3.17 | 2.22 | 3.23 |
| Hake | 3.66–4.32 | 3.59–4.51 | 3.33 | |
| Sardine | 3.16 | 2.99 | 2.98 | |
| Jack mackerel | 2.6 | 3.57 | 3.3 | |
| Chub mackerel | 3.74 | 3.59 | 3.18 | |
| Mesopelagics | 3.49 | 3.12 | | |
| Squat lobster | | | | |
| Humboldt squid | 4.18 | 4.14 | | |
| Euphausiids | 2.50 | 2.12 | 2.12 | |

#### 3.1.2. OSMOSE

After calibrating and hand adjusting the parameters, simulated biomass and landings show a good fit to observed estimates for most of the groups and are stable for at least 300 years (Fig. 9 in the Appendix A). We evaluated the model performance by comparing the trophic levels simulated by OSMOSE (Fig. 2) with literature values (Table 1). The trophic structure in OSMOSE agrees with the trophic structure of Ecopath. After plankton, euphausiids are the lowest trophic level in the simulation, followed by the small pelagic fish. Humboldt squid and hake are the top predators (Fig. 2 and Table 1). For anchovy, Pizarro et al. (2019) observed a trophic level of 3.23 while, in our model, the trophic level of anchovies lies between 3.1 and 3.4. Pizarro et al. (2019) point out the presence of two groups of anchovies with different diet preferences. One of them, with a mean trophic level of 2.91, prefers to graze on phytoplankton and another carnivorous group has a mean trophic level as high as 3.79 (Pizarro et al., 2019). The smaller trophic level range of anchovy in our study is likely due to having a single feeding preference (predator–prey size ratio range) for all schools of the same age class. We could not find trophic level estimations for squat lobster. However, given that it occupies a similar niche to anchovy (Gutiérrez et al., 2008) we may also expect a trophic level around 3. In OSMOSE we observe that it lies between about 2.5 and 3 (Fig. 2).

### 3.2. Effect of plankton temporal variability, accessibility coefficient and larval mortality on fish biomass

The climatological calibration replicates well the time-averaged biomass of fish and macroinvertebrates for the averaged time period 2000–2008 (Fig. 9). For most scenarios and groups, simulated biomass lies within the large variability in the observations (Fig. 3). The hybrid and the interannual configurations show similar results (Fig. 3), pointing out that the different spin-ups do not have a considerable impact on the simulation. This is especially evident for the euphausiids (Fig. 4 right) where both simulations converge after exhibiting different trajectories during the spin-up. This may suggest that the initial conditions are also not so important in OSMOSE once it reaches steady state. When comparing these two experiments with the climatological simulation, the effect of introducing interannual variability in food is evidenced by the appearance of clear interannual fluctuations in euphausiids biomass and an increase in their mean biomass (Fig. 4 right).

When introducing interannual variability in the plankton, most of the simulated higher trophic levels exhibit interannual fluctuations of

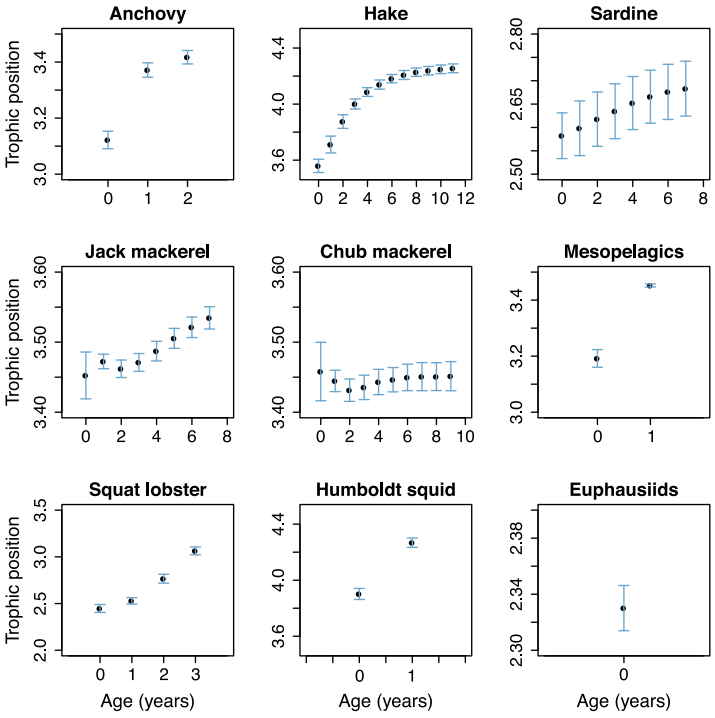


**Fig. 2.** Trophic levels per age class (yearly) of every group simulated by OSMOSE, starting from age-class 0. The mean of 25 years of simulation after spin-up is provided and the error bars indicate the standard deviation.

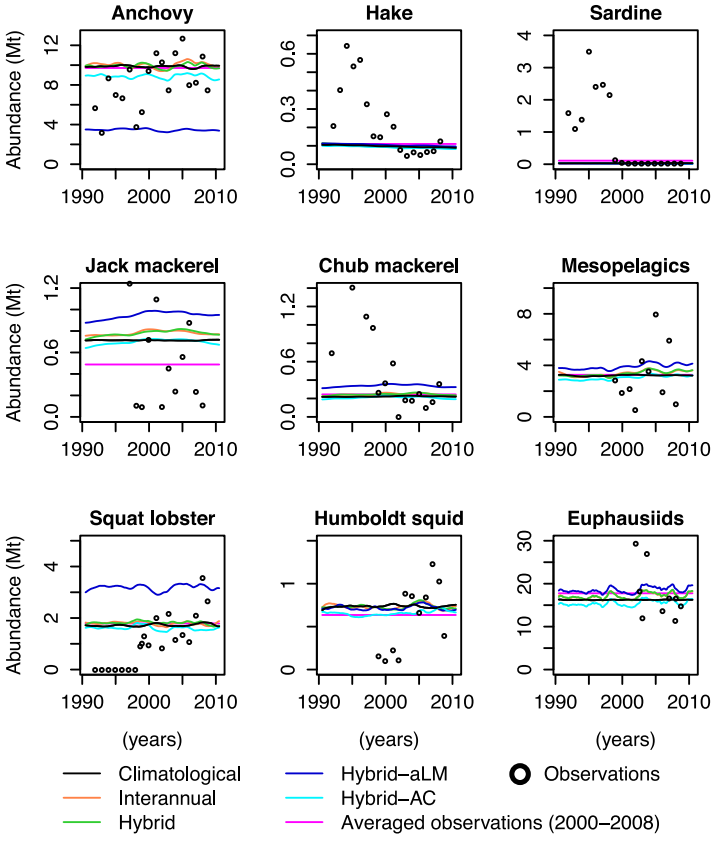


**Fig. 3.** Biomass 12-month running mean after spin-up (see Section 2.4), as well as observations (dots) and 2000 to 2008 averaged observations used to calibrate the model. Observations source: Dimitri Gutierrez, Instituto del Mar del Peru (IMARPE), personal communication. Also available in Oliveros-Ramos et al. (2017), their Fig. 13.

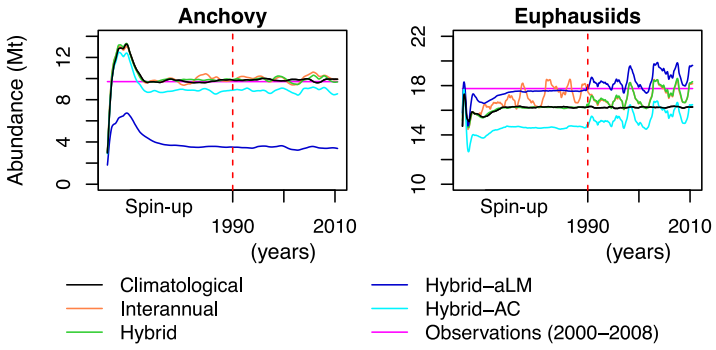


**Fig. 4.** Same as Fig. 3 including spin-up of anchovies and euphausiids.

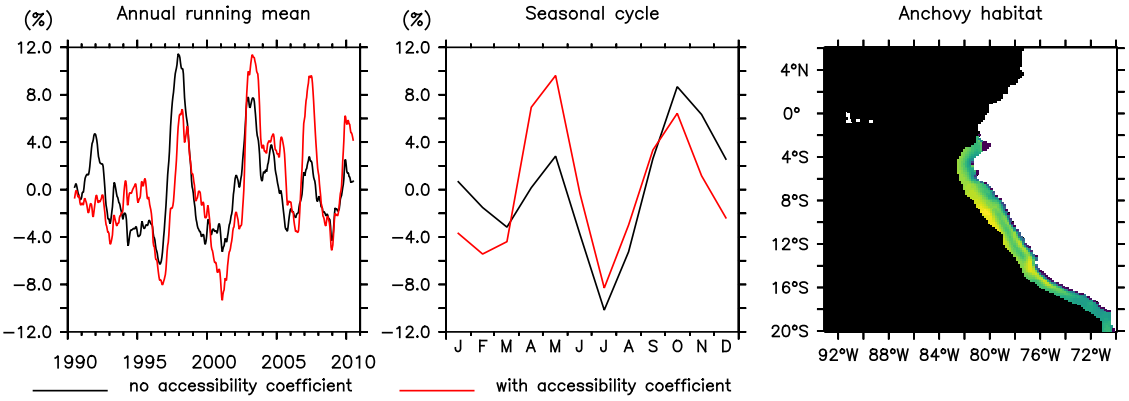


**Fig. 5.** Interannual (left) and seasonal (middle) variability of total plankton in the region occupied by about 90% of anchovies (anchovy habitat in the right panel), calculated taking into account the plankton accessibility coefficient (red) and without plankton accessibility coefficient (black).

about 5 to 10% in their running mean with respect to the climatological set-up (see Appendix A.5). In the hybrid configuration, anchovy and euphausiids exhibit a maximum relative interannual variability of 8.8 and 14.6% of the mean value, respectively. However, in the climatological run, they also exhibit an interannual variability of about 4.1 and 1.1%, respectively. Here we are referring to interannual variability as the difference between the maximum and the minimum of the 12-months running-mean. Therefore, about half of the interannual variability in anchovies comes from the internal dynamics of OSMOSE rather than from the change in plankton forcing. In the case of euphausiids, most of the variability can be directly related to the change in plankton forcing. This is also evident when comparing the hybrid and interannual configuration. Both experiments exhibit almost the same results for the euphausiids, but they differ in the case of anchovies. (Fig. 4). Such difference does not come from the plankton input but rather from the stochasticity and trophic interactions through the foodchain in OSMOSE.

While the hybrid and interannual runs do show a different pattern than the climatological run, their interannual fluctuations tend to be small compared to the high temporal variability in the observations. Other groups show almost no difference between the climatological and the interannual and hybrid configurations. Two important changes in the ecosystem were observed after the El-Niño of 1998: an increase in pelagic squat lobster and a complete collapse of sardines. These are not replicated by the model, which keeps all groups relatively constant before and after the El-Niño (Fig. 3) and highlights the importance of including other sources of temporal variability in end-to-end models, such as species spatial distribution, in addition to food (see Appendix A.5).

We also investigated the importance of total food concentration on fish biomass by reducing the plankton accessibility coefficient (AC) by 10%. The reduction leads to a small decrease in fish biomass (Fig. 3). Both decreasing AC and increasing the LM of anchovy by 10% have a negative impact on anchovy. However, the impact of the LM is much larger than the impact of the AC (Fig. 3). Increasing anchovy LM also affects other species and, in some cases, the impact is also larger than the impact of the decreased AC. Therefore, in this configuration, the LM plays a greater role in controlling the biomass of fish. An extreme case is the squat lobster whose biomass presents little change with decreased AC but almost doubles in the scenario with high anchovy LM (Fig. 3). This evidences the same niche utilisation of the two species.

### 3.3. Further assessment of plankton accessibility coefficient effect on model temporal variability

The plankton accessibility coefficient (AC) is a parameter that scales the plankton available for fish to eat. Because the AC was calibrated for each plankton group individually, its differences across plankton groups (low for large zooplankton and higher for the other groups) might mask the impact of seasonal or temporal variability of plankton on fish. To further investigate this issue, in Fig. 5, we examined the total amount of plankton (i.e., without multiplication by AC), and the variation of plankton as food (after multiplication by AC). For this specific analysis, we focused on the anchovy habitat. Therefore, we isolated the region inhabited by about 90% of the anchovies (Fig. 5 right) as explained in Section 2.2.1. The maximum interannual variability of total plankton in this region is 21 and 18% with and without the calibrated plankton accessibility coefficient, respectively, and the maximum seasonal variability is 18 and 19% (Fig. 5 left and middle). Thus, the interannual variability of total plankton in this region as food is increased by the AC as much as 3%. Furthermore, applying a plankton AC shifts the seasonal peak of highest food availability from October to May (Fig. 5 middle).

Finally, we assessed the effect of applying the same AC to all plankton groups. In OSMOSE, in addition to the AC, the food availability to each fish group is also affected by the predator–prey size ratio, and not

**Table 2**
Euphausiids diet proportions.

| Experiment | $P_S$ | $P_L$ | $Z_S$ | $Z_L$ | others |
|---|---|---|---|---|---|
| Hybrid | 34.3 | 37.4 | 24.4 | 2.9 | 1.0 |
| Hybrid-eqAC | 29.7 | 19.9 | 31.0 | 18.6 | 0.8 |

all plankton groups are preyed by all planktivorous fish. For example, sardines prey on small particles such as plankton while anchovies prefer euphausiids. The temporal variability of plankton comes directly from the biogeochemical model; while euphausiids are explicitly represented in OSMOSE and affected by the variability of their main plankton prey but also the trophic interactions with their predators. Therefore, interspecies competition and predation between species of OSMOSE may also play a role, possibly causing non-linear effects. To further investigate this, in a final experiment (Hybrid-eqAC), we set the AC parameter to a constant value of 10% for every plankton group, thereby omitting any effects caused by the different AC values. For analysis, we focused on the impact of this change on the diet of euphausiids which are the main planktivorous group in OSMOSE and constitute about 85% of the anchovies diet. The large, homogenous AC of 10% increases the contribution of large zooplankton to the diet of euphausiids six times, from only 3% to 18.6% (Table 2). Furthermore, setting up an equal AC for all groups also decreases the direct consumption of large phytoplankton by euphausiids by almost half (Table 2). This group is replaced by small zooplankton as the main prey of euphausiids. This implies that the temporal variability of zooplankton has a greater impact on euphausiids as well as their subsequent predators.

## 4. Discussion

### 4.1. Modelling temporal variability in the NHCS

Our study shows an effect of temporal variability in the biogeochemical model on higher trophic levels (HTL). This variability is similar to the plankton forcing coming from the biogeochemical model. The interannual variability in HTL in OSMOSE is, however, weak compared to the variability in observations and it does not replicate the regime shift after the El-Niño event of 1998. This discrepancy between model and observations may be attributed to several reasons. First, it is possible that the plankton temporal variability in the CROCO-BioEBUS model is, in fact, too weak. The plankton interannual variability observed in our plankton forcing, which is close to 20% of the mean (Section 3.3), is much lower than the variability in anchovy observations. However, compared to satellite data (see Section 3.1.1), the surface chlorophyll in the model displays a similar variability (around 20% of the mean, see Section 3.1.1).

A second reason may be that the link between the biogeochemical model CROCO-BioEBUS and the HTL model OSMOSE is too weak. This link is done only through plankton food forcing for juvenile and adult fish. Other possible links may include the effect of oxygen, temperature and food availability on larval survival and through interannually-varying distribution maps. Temperature and oxygen are some of the variables that were considered when developing the distribution maps for constraining the habitat of the fish (see Oliveros-Ramos, 2014). In Appendix A.5, we provide an alternative configuration where additional interannual variability is introduced by applying interannual distribution maps instead of climatological ones. However, the direct impact of temperature on the physiology of the fish is not considered in OSMOSE. This may be relevant for future developments, especially considering increasing temperatures due to climate change (see Penn and Deutsch, 2022). Metabolic needs of swimming against currents and non-random movement of individual schools, such as searching for food and avoiding predators, are also not considered in the model. This proved to be relevant in the modelling study by Watson et al. (2015).

It may also be that in the real ocean, there is not a straightforward bottom-up control of HTL as supported by Ayón et al. (2004). They found no significant correlation between zooplankton and anchovy observations off Peru between the period of 1984 to 2001, pointing to other potential drivers than food production. Therefore, the main driver of the interannual variability in the NHCS might not be as simple as adult fish following the trends in plankton food. This may be a peculiarity of the NHCS that makes the modelling of this ecosystem so challenging. Simulating environmental variability in OSMOSE only through changes in plankton food for juvenile and adult fish has, in fact, produced stronger impacts in other ecosystems. Fu et al. (2012) evaluated the effects of interannual variability in plankton input on their OSMOSE model configuration for the Strait of Georgia in British Columbia, Canada. In their study, interannual variability in phytoplankton produced strong effects of more than ±50% on their small forage fish, herring (Fu et al., 2012, their Figure 5a). This is much larger than the response observed in our study. In contrast, interannually-varying plankton in our study produces a change of about 5 to 10% in the biomass of most of the simulated HTL groups (see Appendix A).

Fourthly, the period simulated in the NHCS is, rather than a steady-state-El-Niño-new-steady-state setting, a part of a longer trend of interannual and multidecadal fluctuations in the ecosystem. Anchovy and sardine have been the two small pelagic fish fisheries with the highest catches since the 1960s. These fishes fluctuate over the years with periods dominated by anchovies and others by sardines (Chavez et al., 2003). The period from 1990 to 2010 corresponds to a progressive decrease of sardines and an overtake by anchovies. To simulate these fluctuations, a longer timeseries would be necessary. This, however, is limited by the availability of data.

Furthermore, while our configuration includes the biggest pelagic, macroinvertebrate and demersal fisheries off Peru (PRODUCE, 2013), it may require other ecosystem components to account for the main drivers affecting these fisheries. As a demersal species, hake feeds on both pelagic and benthic fish species as well as euphausiids (Ware, 1992). However, in our configuration, we only accounted for pelagic prey. Hence, the variability in this species is missing the effects of its benthic prey. In addition, a possible explanation for the high production of the NHCS is the resetting of the system every few years by El-Niño events that impact both forage fish and their predators. Since higher trophic levels usually have longer generation times and take longer to recover, this opens a loophole for forage fish to dominate the succession (Bakun and Broad, 2003; Bertrand et al., 2004). However, we are missing apex predators in OSMOSE. The top predators in our configuration are the Humboldt squid and the demersal fish hake but we are missing other groups such as marine mammals and sharks. Taylor et al. (2008) achieved some level of interannual variability in an Ecopath with Ecosim configuration of the NHCS utilising a fit-to-time-series routine that evaluated different predator–prey interactions, emphasising the importance of trophic dynamics. Their configuration included, among other animals, seabirds, chondrichthyans, cetaceans and pinnipeds. While not containing as many groups as Ecopath, OSMOSE, in contrast, allows for a detailed spatial representation of species with explicit life cycles, and can take input from a biogeochemical model with finely resolved nutrient cycles.

Finally, the representation of survival of larvae may be of fundamental importance. To our knowledge, the study by Oliveros-Ramos et al. (2017) is the only modelling project with OSMOSE that has successfully replicated the regime shift after the El-Niño event of 1998. They achieved this, in addition to including interannual distribution maps, by calibrating time-varying parameters. While such an approach successfully replicates the interannual variability in the system, it masks the interactions between the biogeochemistry and HTL because the temporally varying model parameters account for all temporal variability, which is not necessarily justified, not allowing to pinpoint processes. For instance, in Oliveros-Ramos et al. (2017, their Figure 10), anchovy larval mortalities (LM) fluctuated more than 2-fold around the

**Table 3**
Comparison of survival rates (dimensionless) during egg and larval stages (period of estimation provided in days) in three species of our configuration and species in the same genera provided by Dahlberg (1979, their Tables 1 and 2). Species provided by Dahlberg (1979): Anchovy, *Engraulis japonica* (Nakai et al., 1955); Jack mackerel, *Trachurus symmetricus* (Farris, 1961); sardine, Pacific sardine (Murphy, 1961, scientific name not provided). The relationship between the daily larval mortality (LM/15 days = $\mu$) and survival ($S$) in OSMOSE is given by $S = \frac{N(t+\Delta t)}{N(t)} = e^{-\mu \Delta t}$ (using the exponential approach provided in OSMOSE source code: https://github.com/osmose-model/osmose/tree/master/java [Accessed: 2021-10-28]).

| | Species | Anchovy | Sardine | Jack mackerel |
|---|---|---|---|---|
| Dahlberg (1979) | Period of estimation (days) | 31 | 50 | 57 |
| | Survival per day | 0.799 | 0.883 | 0.83 |
| OSMOSE | Period of estimation (days) | 15 | 15 | 15 |
| | Survival per day | 0.555 | 0.461 | 0.524 |

central value. In our study, we found that OSMOSE is very sensitive to the value of LM, with only a 10% change decreasing the biomass of anchovy by more than half. The impact is much stronger than the effect caused by a 10% decrease in available food. This suggests that the key to reproduce the interannual variability of the fisheries in the NHCS may not be in the food provided to adults but rather on the survival of larvae.

### 4.2. Towards a better parameterisation of larval mortality

Understanding the drivers of recruitment is essential to assess the growth of a population and, in turn, its maximum sustainable yield. The maximum sustainable yield is the maximum amount of fish that can be taken from the system while keeping the population growth at sustainable levels. Past studies emphasise the importance of recruitment and mortality on the growth rate of fish populations (Tsikliras and Froese, 2019). In OSMOSE, recruitment is affected by the mortality of larvae. Therefore, in this section, we discuss the larval mortality in OSMOSE and how to improve its parameterisation.

Sources of larval mortality can be divided in four categories: (1) mortality related to parents condition and variability among eggs (2) abiotic factors such as temperature (3) starvation and (4) predation. Predation (4) is already explicitly included in OSMOSE. The other factors are represented by the larval mortality parameter (LM) which accounts for mortality during the first 15 days of life of eggs and larvae. It intends to account for processes that happen during the earliest life stages of fish when mortality is very high but hard to estimate from empirical studies. For instance, spatio-temporal match between larvae and plankton allows fish recruitment (Cushing, 1990). In upwelling regions, this occurs at an optimal wind stress (Cury and Roy, 1989; Cushing, 1990). In this way, the LM parameter in OSMOSE also accounts for the impact of environmental processes on larvae such as wind-dependence mixing. Our OSMOSE configuration proved to be highly sensitive to the LM parameter. Following the setting-up of other OSMOSE configurations (e.g., Vergnon et al., 2008; Marzloff et al., 2009; Travers et al., 2009; Fu et al., 2012; Grüss et al., 2015; Halouani et al., 2016), we estimated this parameter during the calibration process of the model. Therefore, it was used, in combination with the plankton accessibility coefficient (AC), to adjust the fish biomass to observed levels. Alternatives to calibrating this parameter may include to find a mechanistic representation of the fine scale larvae dynamics in relation to the physical environment and food availability. This could resolve starvation (3) and abiotic causes of mortality (2), leaving only causes related to individual variability (1) to be calibrated.

In Table 3, we compare survival, derived from larval mortalities, of sardine, jack mackerel and anchovy against values provided by Dahlberg (1979). The daily survival rates in OSMOSE are smaller than in Dahlberg (1979) (Table 3). However, this comparison has to be taken with caution since the egg and first-feeding larvae period in OSMOSE (15 days) is shorter than the periods reported by Dahlberg (1979) (Table 3). Therefore, the high mortality of the initial days of life of fish is concentrated over a shorter timeframe and it is not surprising that the survival rates are lower.

Finding a mechanistic link between the LM and the environmental drivers will be a crucial step in the development of end-to-end models. Roy (1993) found a relationship between wind speed and recruitment of anchovy and sardine populations in several eastern boundary upwelling systems. This is based on the hypothesis that low wind and upwelling is linked to low primary productivity and recruitment; high wind-speeds, on the other hand, generates strong mixing that disperses larvae away from the food. Therefore, there is an "Optimal Environmental Window" (Cury and Roy, 1989) where the wind is neither too strong, nor too weak and maximum recruitment is achieved (Roy, 1993). From a modelling perspective, Lett et al. (2008) proposed an explicit simulation of the larval stages of fish as a Lagrangian individual-based model with salinity, temperature and velocity inputs. A simple experiment to increase the effect of food availability on fish in OSMOSE is to link the LM to the food availability through a linear relationship. Other potential improvements for the larval parameterisation in OSMOSE may include to either link the LM parameter to environmental conditions, for instance, through the relationship found by Roy (1993); or to include a whole new larval sub-model in OSMOSE, similar to the one proposed by Lett et al. (2008). Brochier et al. (2008) simulated anchovy larval survival off the coast of Peru based on a hydrodynamic model simulating larval drift and also considering lethal temperature, egg buoyancy and active vertical swimming of the larvae. The temporal dynamics of their results roughly resemble the seasonality in observations. While no interannual variability was taken into account, this approach shows potential for resolving larval dynamics in a mechanistic way. The time-series of estimated larval mortalities by Oliveros-Ramos et al. (2017) provides a good fitting hindcast. A statistical relationship with the physical parameters and traces of the biogeochemical model could then be derived to produce estimates for future projections. This may not only reduce the uncertainty in the LM but, because LM and AC act in opposite directions, it would potentially also provide insights into better estimations of the AC during the calibration process by reducing the number of parameters to be optimised.

There is no model that fits all purposes but models are useful tools to investigate certain questions. Every question, however, poses specific requirements for the model. OSMOSE was originally developed to investigate trophic interactions among HTL such as fish (Shin and Cury, 2001, 2004). At this time, fish schools were divided into piscivorous and non-piscivorous fish and their maximum populations were regulated by a carrying capacity (Shin and Cury, 2001, 2004). Later on, it was modified to also include explicit food forcing from plankton groups (Travers, 2009) which could be derived from satellite and surveys data (Marzloff et al., 2009) or biogeochemical models (Travers et al., 2009). At this point, a carrying capacity parameter was not necessary anymore since limited resources were explicitly modelled. However, the AC was implemented to scale the biomass of plankton that is available to the fish. The reasoning behind is that not all plankton in the water-column is available for the fish to feed (Travers et al., 2009). This parameter is, however, poorly understood and it is usually calibrated. A blind calibration of the AC may, however, obscure

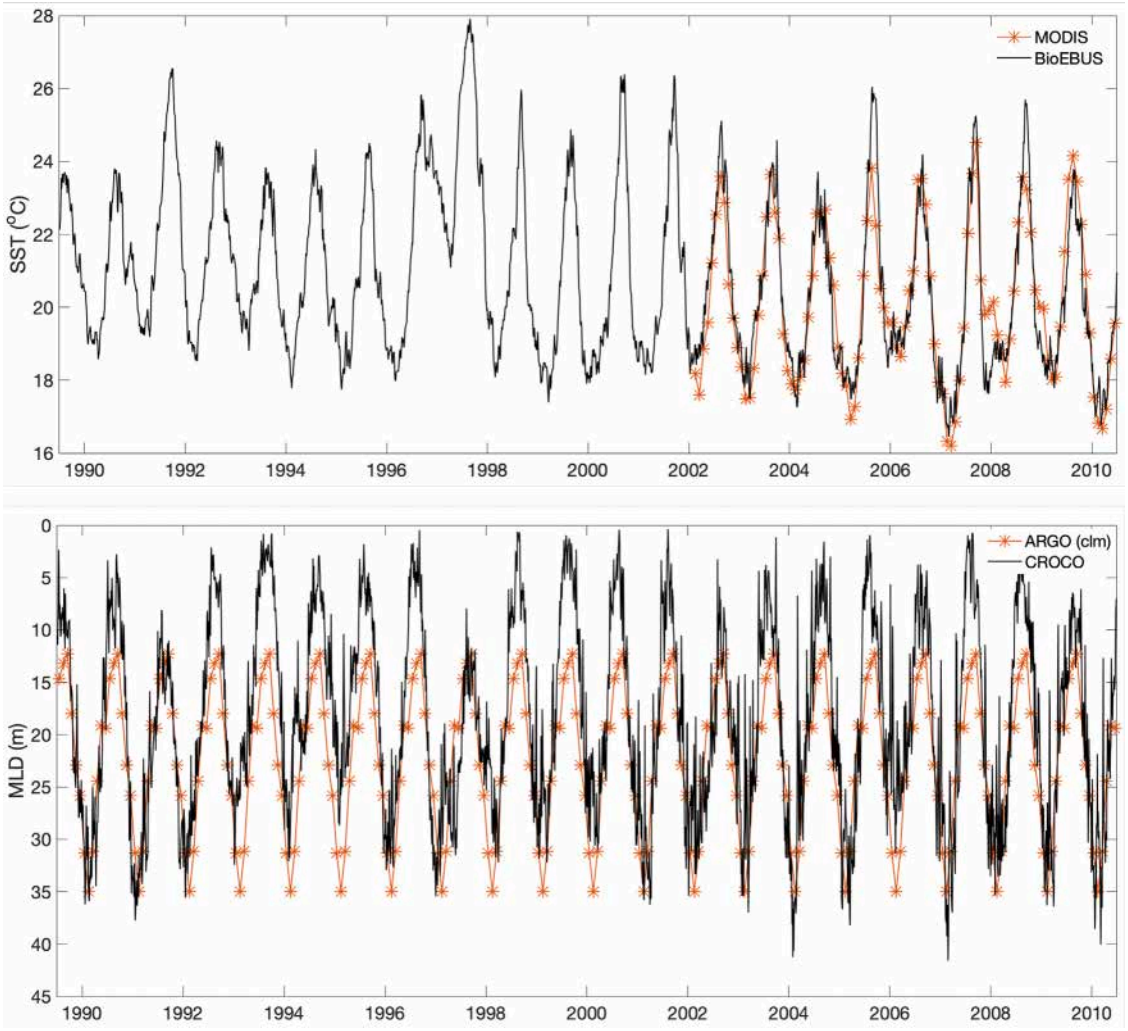


**Fig. 6.** Sea surface temperature (SST) and mixed layer depth (MLD) averaged over the closest 2° or about 200 km off the coast of Peru from 15 to 5°S. Top: SST in the model (black) and in MODIS observations (red; https://oceancolor.gsfc.nasa.gov/l3/ [Accessed: 2022-07-24]). Bottom: Simulated MLD (black) compared with climatological observations of temperature threshold mean MLD (red) by Holte et al. (2017).

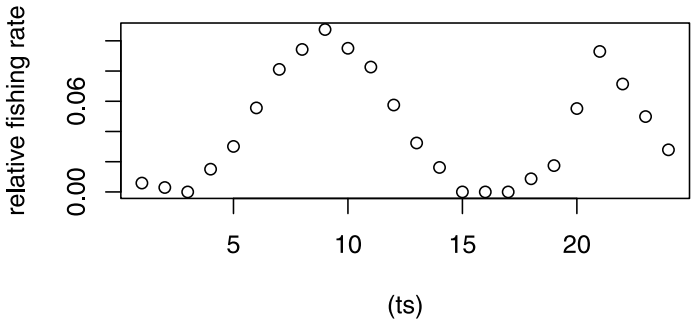


**Fig. 7.** Seasonal variability in the fishing rate. The sum of all points for 24 time-steps in one year is 1. These were calculated from monthly landings data provided by Gutierrez-Aguilar and Instituto del Mar del Peru (IMARPE) (personal communication).

the interactions between higher and lower trophic levels in the end-to-end model. The study by Travers-Trolet et al. (2014b,a) looked at the combined effects of top-down and bottom-up pressures on a two-way coupled $N_2P_2Z_2D_2$-OSMOSE model system. The fish-to-plankton feedback was achieved by calculating a mortality map of plankton based on the consumption by fish. The maximum consumption of every plankton group was given by the AC which came from a calibration. Since, in a two-way coupling system, fish consumption has a direct impact on zooplankton mortality, the AC might also affect the biogeochemistry of

**Table 4**
Parameters. Species and groups are: a for anchovy, h for hake, s for sardine, jm for jack mackerel, chm for chub mackerel, m for mesopelagics, sl for squat lobster, hs for Humboldt squid, e for euphausiids. For a detailed explanation on each parameter please refer to Shin and Cury (2004), as well as the official OSMOSE documentation: http://documentation.osmose-model.org/index.html [Accessed: 2021-10-28].
*Source:* Oliveros-Ramos and Lujan-Paredes, personal communication, based on the configuration by Oliveros-Ramos et al. (2017).

| Parameter | Unit | a | h | s | jm | chm | m | sl | hs | e |
|---|---|---|---|---|---|---|---|---|---|---|
| simulation.ncschool | n | 24 | 12 | 12 | 24 | 12 | 148 | 4 | 48 | 148 |
| species.linf | cm | 19.5 | 68 | 38.71 | 81.6 | 40.6 | 8 | 4.2 | 95 | 2.6 |
| species.K | 1/yr | 0.76 | 0.,025 | 0.22 | 0.,167 | 0.41 | 1.15 | 0.,375 | 1.1 | 1.8 |
| species.t0 | years | −0.14 | −0.,269 | −1.34 | −0.28 | −0.05 | −0.06 | −328 | −0.09 | −198 |
| species.vonbertalanffy.threshold.age | years | 0.35 | 0.5 | 0.5 | 0.5 | 0.5 | 0.35 | 0.5 | 1 | 0.1 |
| species.length2weight.condition.factor | g/cm | 0.0065 | 0.,007 | 0.0089 | 0.0135 | 0.0086 | 0.00832 | 0.,174 | 0.,005 | 0.00925 |
| species.length2weight.allometric.power | – | 3 | 3.05 | 2.99 | 2.9248 | 3.26 | 3.15 | 3.03 | 3.4 | 3 |
| species.relativefecundity | – | | | | | 1 | | | | |
| species.egg.size | cm | | | | | 0.1 | | | | |
| species.egg.weight | g | | | | | 0.0005386 | | | | |
| species.sexratio | – | 0.5 | 0.5 | 0.5 | 0.5 | 0.5 | 0.5 | 0.5 | 0.5 | 0.5 |
| species.maturity.size | cm | 12 | 35 | 21 | 29 | 29 | 2.5 | 1.9 | 66 | 0.8 |
| species.lifespan | years | 3 | 12 | 8 | 8 | 10 | 2 | 4 | 1.5 | 1 |
| mortality.starvation.rate.max | 1/ts | 1 | 0.05 | 0.1 | 0.15 | 0.05 | 0.5 | 0.1 | 0.1 | 0.5 |
| predation.efficiency.critical | – | 0.57 | 0.57 | 0.57 | 0.57 | 0.57 | 0.57 | 0.57 | 0.57 | 0.57 |
| predation.ingestion.rate.max | g food/ g fish/ year | 3.5 | 3.5 | 3.5 | 3.5 | 3.5 | 3.5 | 3.5 | 3.5 | 3.5 |
| predation.predPrey.sizeRation.max | – | 8, 6 | 3, 2.5 | 25, 150 | 20, 15 | 20, 15 | 3.5 | 2 | 2.5, 2, 1 | 15, 10 |
| predation.predPrey.sizeRation.min | – | 800, 200 | 50, 50 | 1000, 10000 | 300, 200 | 300, 200 | 100 | 150 | 35, 55, 70 | 3000, 2000 |
| predation.predPrey.stage.threshold | cm | 10 | 18 | 13 | 20 | 20 | – | – | 30, 60 | 0.6 |
| movement.distribution.method | – | | | | | maps | | | | |
| movement.randomwalk.range | cells/ts | | | | | 1 | | | | |
| mortality.algorithm | – | | | | | stochastic | | | | |
| mortality.fishing.recruitment.size | cm | 12 | 35 | 21 | 26 | 26 | 2.5 | 1.9 | 30 | 0.8 |
| mortality.natural.rate[a] | 1/yr | 0.34 | 0.3 | 0.3[c] | 0.24 | 0.25 | 1.19 | 0.3 | 6.27 | 0.954[b] |
| mortality.fishing.rate[a] | 1/yr | 1.1 | 0.3 | 0.4 | 0.3 | 0.5 | 0 | 0 | 0.11[c] | 0 |
| mortality.natural.larva.rate[d] | 1/ts | 8.83 | 9.63 | 11.6[c] | 9.7 | 9.16 | 4.63 | 0.61 | 4.47 | 2.6 |
| mortality.subdt[c] | n | | | | | 10 | | | | |
| osmose.version | – | | | | | Osmose 3 Update 3 Release 3 (2018/11/28) | | | | |
| ltl.java.classname | – | | | | | fr.ird.osmose.ltl.LTLFastForcing | | | | |
| grid.java.classname | – | | | | | fr.ird.osmose.grid.OriginalGrid | | | | |
| predation.predPrey.stage.structure | – | | | | | size | | | | |
| predation.accessibility.structure | – | | | | | size | | | | |
| q-factor (see main text) | – | 0.87 | 0.41 | 0.74 | 0.54 | 0.76 | 0.16 | 0.88 | 0.31 | 0.5 |
| population.seeding.biomass | (tons) | $8 \times 10^6$ | $2.1 \times 10^5$ | $1 \times 10^4$[c] | $4.36 \times 10^6$ | $9 \times 10^5$ | $1.5 \times 10^7$ | $1 \times 10^7$ | $3 \times 10^6$ | $4 \times 10^7$ |

[a] Marzloff et al. (2009).
[b] Tam et al. (2008).
[c] Adjusted.
[d] Calibrated.

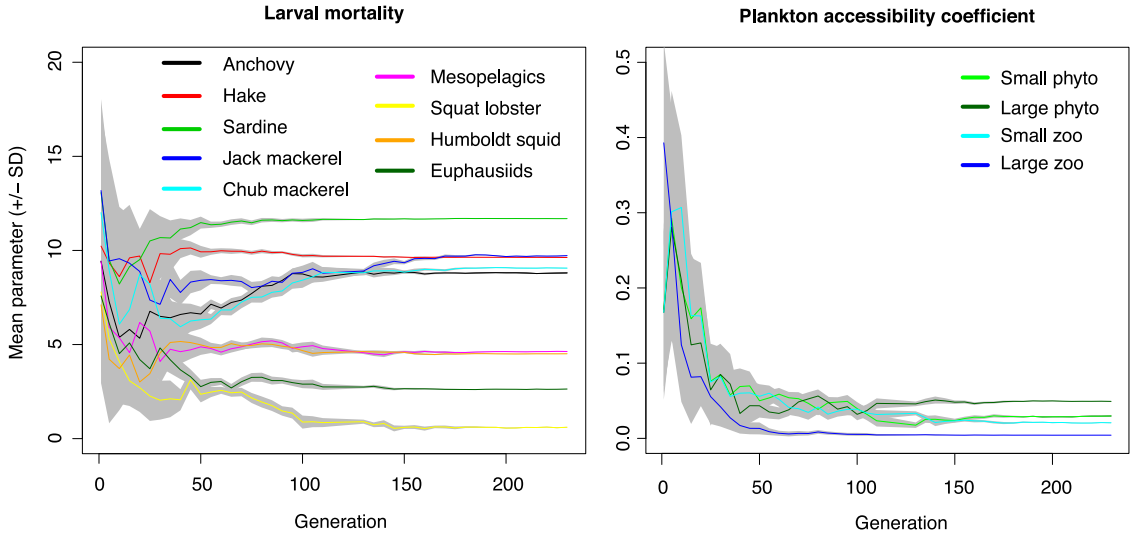


**Fig. 8.** Mean plankton accessibility coefficient (dimensionless), larval mortality (1/ts) and their standard deviation (shaded area) of the parameters in the 75 individuals of the calibration.

the model. Therefore, special attention has to be taken for the choice of this parameter.

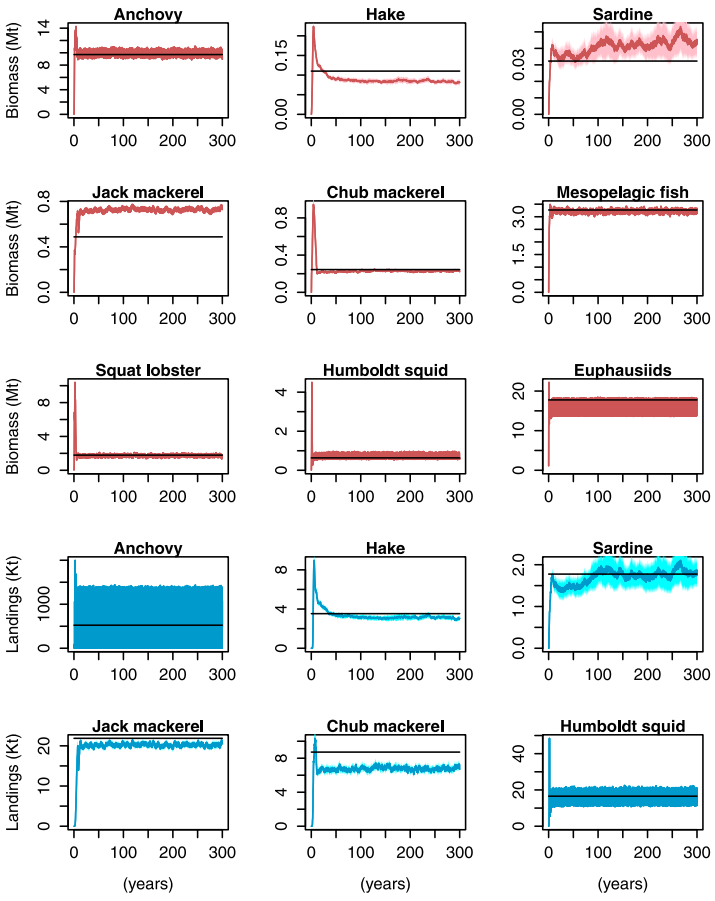


**Fig. 9.** Simulated biomass (red) and monthly landings (blue) over 300 years of climatological simulation and observations averaged from 2000 to 2008 (black). These were the observations used to calibrate the model and the model output with the final set of calibrated and adjusted parameters.

## 5. Conclusion

We set up a climatological configuration for the Northern Humboldt Current System, coupling the higher trophic levels model OSMOSE with the physical–biogeochemical model CROCO-BioEBUS. The calibrated model replicates well the mean biomass between 2000 and 2008 of most of the groups in a steady state. Changing the climatological plankton forcing to an interannual time-series introduces temporal variability in the ecosystem. However, it does not replicate the strong fluctuations in fish, especially sardine and anchovy, observed before and after the El-Niño event of 1998. The inability of our model to replicate the regime shift may arise from the period between 1990 and 2010 not being in a steady state, like our configuration, but being a transitionary state from a sardine to an anchovy-dominated regime. Covering a longer time-series might help to capture longer-term fluctuations. In addition, other processes should be assessed as potential major drivers of variability. Temporal changes in the habitat of fish may be an additional source of interannual variability. These were included by Oliveros-Ramos et al. (2017) as interannually-varying distribution maps based on statistical methods. In climate projections, these could be directly linked to the variables in the ocean-circulation-biogeochemical model. Linking other environmental drivers, for instance temperature and oxygen, with life stages of higher trophic levels, for instance larvae, may shed light into the main causes of the strong fluctuations of small pelagic fish in the Northern Humboldt Current System. This, in turn, may reduce the uncertainty in the plankton accessibility coefficient which is the most poorly constrained parameter in OSMOSE. When the main goal of using OSMOSE is to explore the interactions between higher trophic levels and biogeochemistry, including plankton, we recommend a thoughtful consideration of what the plankton accessibility coefficient represents in the model. For example, some of the large zooplankton may perform vertical migrations and hide in the oxygen minimum zone. In this case, it would not be available for the fish during part of the day and it would require a different accessibility coefficient. However, if this information is missing while parameters need to be calibrated, for evaluating the link between the biogeochemical processes and OSMOSE, we recommend to calibrate the same accessibility coefficient for all plankton groups.

## CRediT authorship contribution statement

**Mariana Hill Cruz:** Conceptualization, Methodology, Formal analysis, Writing. **Ivy Frenger:** Supervision, Writing. **Julia Getzlaff:** Conceptualization, Supervision, Writing. **Iris Kriest:** Conceptualization, Supervision, Writing. **Tianfei Xue:** Methodology, Writing. **Yunne-Jai Shin:** Supervision, Writing.

## Declaration of competing interest

The authors declare that they have no known competing financial interests or personal relationships that could have appeared to influence the work reported in this paper.

## Data availability

The model code and output are available on request. For requests regarding the observational data used to calibrate the model, we refer to IMARPE which provided this data.

## Acknowledgements

This study was funded by the Bundesministerium für Bildung und Forschung (BMBF), Germany through the projects: Coastal Upwelling System in a Changing Ocean CUSCO (03F0813 A) and Humboldt-Tipping (01LC1823B). In addition, JG received funancial support by the BMBF funded project CO2Meso (03F0876A) and TX by the China Scholarship Council (201808460055). Simulations and model calibration were carried out using the computing facilities of the Norddeutscher Verbund zur Förderung des Hoch- und Höchstleistungsrechnens – HLRN.

We thank Ricardo Oliveros-Ramos and Criscely Luján-Paredes for providing the OSMOSE Humboldt interannual configuration and distribution maps. We also thank Ricardo Oliveros-Ramos for providing scientific advice and technical support to this project. We thank Nicolas Barrier for his technical support to the project. We thank the Instituto del Mar del Perú (IMARPE) for providing the data to calibrate the model and we thank Dimitri Gutierrez for facilitating this data. Finally, we thank Andreas Oschlies for his helpful contribution to the discussion, and two anonymous reviewers for their valuable comments to improve the manuscript.

## Appendix A

### A.1. CROCO sea surface temperature and mixed layer depth

The model sea surface temperature (SST) resembles well satellite observations from 2002 to 2010 (Fig. 6 top). The SST increases during El-Niño event of 1997–1998 in comparison to the rest of the time series (Fig. 6 top). The mixed layer depth becomes deeper during El-Niño event of 1997–1998 (Fig. 6 bottom).

### A.2. Higher trophic levels model parameters

Table 4 provides the parameters used to run OSMOSE. The original name of each parameter as it is read by the model is provided. Fig. 7 provides the seasonality of the anchovy landings. Additional parameters and the distribution maps are provided in the Supplement.

### A.3. Calibration evolution

The calibration ran for 400 generations using 75 individuals. The global fitness function evolved from an original global fitness of 521.59 on the first generation, to 0.29 on generation 200. From here, it only decreased to 0.26 at generation 400. Fig. 8 shows the evolution of the parameter sets over the first half of the calibration.

### A.4. Climatological configuration

Fig. 9 shows biomass and landings in the climatological configuration of OSMOSE over a 300 years run. The model resembles well averaged observations against which it was optimised.

### A.5. Configuration with interannual distribution maps

In this section we provide the relative variability with respect to the climatological configuration (see Section 2.4). We also examine the hybrid configuration (see Section 2.4) running with interannually-varying distribution maps from 1992 to 2008 instead of climatological distribution maps. The initialisation, food forcing and parameters are the same as in the hybrid configuration. The interannual distribution maps are the same as used by Oliveros-Ramos et al. (2017). For most

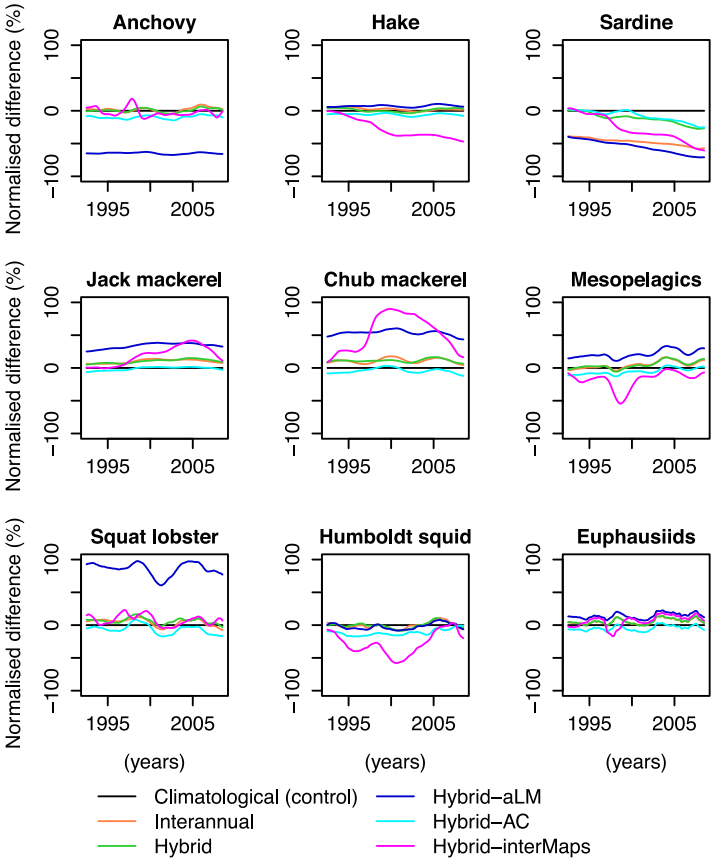


**Fig. 10.** Normalised difference between the 12-month running mean of the control (climatological configuration) and the other experiments (see Section 2.4). We also included a hybrid configuration with interannual distribution maps from 1992 to 2008 (Hybrid-interMaps).

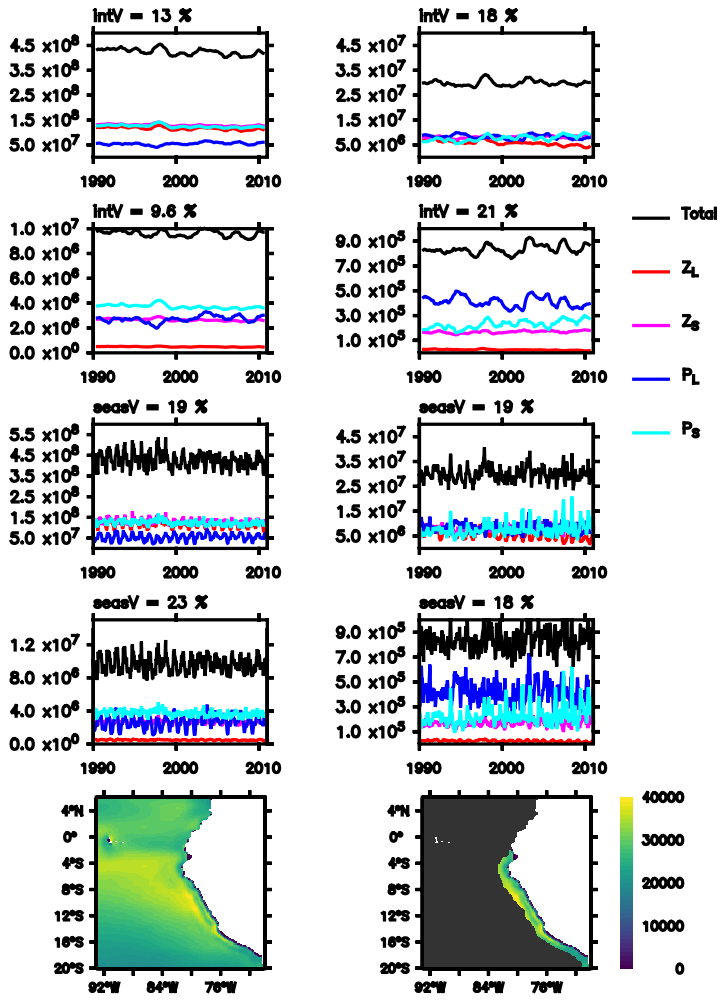


**Fig. 11.** Rows top to bottom: annual running mean of plankton, annual running mean of plankton multiplied by their respective accessibility coefficients, plankton time-series multiplied by their respective accessibility coefficients (tonnes) and time-averaged total plankton (tonnes per grid cell). intV and seasV refer to the relative difference between the maximum and minimum of the annual running mean and the seasonal cycle, respectively. Columns: plankton in the whole domain (left) and plankton in the region where 90% of the anchovies live.

groups, introducing interannual variability in plankton produces a relative change of around 5 to 10% (Fig. 10). Changing the larval mortality of anchovy in addition to the interannual variability in plankton has a larger impact in all groups, except for the Humboldt squid, than only introducing interannual variability in the plankton (Fig. 10). Applying interannual variability to the distribution maps has a visible impact on the fish when compared to using climatological maps (Fig. 10). Compared to the hybrid configuration, in the configuration with interannual maps, some of the groups, for instance Humboldt squid, exhibit a stronger interannual variability (Fig. 10). In all experiments but the climatological set-up, sardines get destabilised and exhibit a continuous decline throughout the time-series (Fig. 10).

### *A.6. Plankton interannual and seasonal variability*

Plankton has interannual and seasonal variability. These are highly affected by the accessibility coefficient (intV = 13% and 9.1% and seasV = 19% and 27%, Fig. 11) in the full domain. On the other hand, the accessibility coefficient has a smaller effect when considering only the anchovy habitat (see Section 3 for a description of the anchovy habitat; intV and seasV differences are only 3 and 1%, respectively, Fig. 11).

## Appendix B. Supplementary data

Supplementary material related to this article can be found online at https://doi.org/10.1016/j.ecolmodel.2022.110097.

## References

Alheit, J., Niquen, M., 2004. Regime shifts in the Humboldt current ecosystem. Prog. Oceanogr. 60 (2-4), 201–222. http://dx.doi.org/10.1016/j.pocean.2004.02.006.

Aranda, M., 2009. Evolution and state of the art of fishing capacity management in Peru: The case of the anchoveta fishery. Pan-Am. J. Aquat. Sci. 4 (2), 146–153.

Ayón, P., Purca, S., Guevara-Carrasco, R., 2004. Zooplankton volume trends off Peru between 1964 and 2001. ICES J. Mar. Sci. 61 (4), 478–484. http://dx.doi.org/10.1016/j.icesjms.2004.03.027.

Bakun, A., Broad, K., 2003. Environmental 'loopholes' and fish population dynamics: comparative pattern recognition with focus on El Niño effects in the Pacific. Fisheries Oceanography 12 (4–5), 458–473. http://dx.doi.org/10.1046/j.1365-2419.2003.00258.x.

Bănaru, D., Diaz, F., Verley, P., Campbell, R., Navarro, J., Yohia, C., Oliveros-Ramos, R., Mellon-Duval, C., Shin, Y.-J., 2019. Implementation of an end-to-end model of the Gulf of lions ecosystem (NW Mediterranean Sea). I. Parameterization, calibration and evaluation. Ecol. Model. 401, 1–19. http://dx.doi.org/10.1016/j.ecolmodel.2019.03.005.

Barber, R.T., Chavez, F.P., 1983. Biological consequences of El Niño. Science 222 (4629), 1203–1210. http://dx.doi.org/10.1126/science.222.4629.1203.

Barrett, R.C., Caulkins, J.P., Yates, A.J., Elliott, D., 1985. Population dynamics of the Peruvian anchovy. Math. Model. 6 (6), 525–548. http://dx.doi.org/10.1016/0270-0255(85)90052-1.

Bertrand, A., Segura, M., Gutiérrez, M., Vásquez, L., 2004. From small-scale habitat loopholes to decadal cycles: a habitat-based hypothesis explaining fluctuation in pelagic fish populations off Peru. Fish and Fisheries 5 (4), 296–316. http://dx.doi.org/10.1111/j.1467-2679.2004.00165.x.

Boerema, L.K., Gulland, J.A., 1973. Stock assessment of the Peruvian anchovy (Engraulis ringens) and management of the Fishery. J. Fish. Res. Board Can. 30 (12), 2226–2235. http://dx.doi.org/10.1139/f73-351.

Brochier, T., Lett, C., Tam, J., Fréon, P., Colas, F., Ayón, P., 2008. An individual-based model study of anchovy early life history in the northern Humboldt current system. Prog. Oceanogr. 79 (2-4), 313–325. http://dx.doi.org/10.1016/j.pocean.2008.10.004, The Northern Humboldt Current System: Ocean Dynamics, Ecosystem Processes, and Fisheries.

Carr, M.-E., 2002. Estimation of potential productivity in eastern boundary currents using remote sensing. Deep Sea Res. II 49 (1-3), 59–80. http://dx.doi.org/10.1016/S0967-0645(01)00094-7.

Carton, J.A., Chepurin, G.A., Chen, L., 2018. SODA3: A new ocean climate reanalysis. J. Clim. 31 (17), 6967–6983. http://dx.doi.org/10.1175/JCLI-D-18-0149.1.

Chavez, F.P., Bertrand, A., Guevara-Carrasco, R., Soler, P., Csirke, J., 2008. The northern Humboldt current system: Brief history, present status and a view towards the future. Prog. Oceanogr. 79 (2-4), 95–105. http://dx.doi.org/10.1016/j.pocean.2008.10.012.

Chavez, F.P., Messié, M., 2009. A comparison of eastern boundary upwelling ecosystems. Prog. Oceanogr. 83 (1–4), 80–96. http://dx.doi.org/10.1016/j.pocean.2009.07.032.

Chavez, F.P., Ryan, J., Lluch-Cota, S.E., Ñiquen, M., 2003. From anchovies to sardines and back: multidecadal change in the Pacific ocean. Science 299 (5604), 217–221. http://dx.doi.org/10.1126/science.1075880.

Christensen, V., de la Puente, S., Sueiro, J.C., Steenbeek, J., Majluf, P., 2014. Valuing seafood: The Peruvian fisheries sector. Mar. Policy 44, 302–311. http://dx.doi.org/10.1016/j.marpol.2013.09.022.

Cury, P., Roy, C., 1989. Optimal environmental window and pelagic fish recruitment success in upwelling areas. Can. J. Fish. Aquat. Sci. 46 (4), 670–680. http://dx.doi.org/10.1139/f89-086.

Cushing, D., 1990. Plankton production and year-class strength in fish populations: An update of the match/mismatch hypothesis. In: Blaxter, J., Southward, A. (Eds.), In: Advances in Marine Biology, vol. 26, Academic Press, pp. 249–293. http://dx.doi.org/10.1016/S0065-2881(08)60202-3.

Dahlberg, M.D., 1979. A review of survival rates of fish eggs and larvae in relation to impact assessments. Mar. Fish. Rev. 41.

Diaz, F., Bănaru, D., Verley, P., Shin, Y.-J., 2019. Implementation of an end-to-end model of the Gulf of Lions ecosystem (NW Mediterranean Sea). II. Investigating the effects of high trophic levels on nutrients and plankton dynamics and associated feedbacks. Ecol. Model. 405, 51–68. http://dx.doi.org/10.1016/j.ecolmodel.2019.05.004.

Duboz, R., Versmisse, D., Travers, M., Ramat, E., Shin, Y.-J., 2010. Application of an evolutionary algorithm to the inverse parameter estimation of an individual-based model. Ecol. Model. 221 (5), 840–849. http://dx.doi.org/10.1016/j.ecolmodel.2009.11.023.

FAO, 2020. The State of World Fisheries and Aquaculture 2020. Sustainability in action. ISBN: 978-92-5-132692-3, http://dx.doi.org/10.4060/ca9231en, FAO, Rome.

Farris, D., 1961. Abundance and distribution of eggs and larvae of jack mackerel (*Trachurus symmetricus*). Fish. Bull. US. 61, 247–279.

Fu, C., Shin, Y., Perry, R., King, J., Liu, H., 2012. Exploring climate and fishing impacts in an ecosystem model of the strait of Georgia, British Columbia. In: Global Progress in Ecosystem-Based Fisheries Management. Alaska Sea Grant, University of Alaska Fairbanks, pp. 65–86. http://dx.doi.org/10.4027/gpebfm.2012.04.

Fulton, E.A., 2010. Approaches to end-to-end ecosystem models. J. Mar. Syst. 81 (1-2), 171–183. http://dx.doi.org/10.1016/j.jmarsys.2009.12.012, Contributions from Advances in Marine Ecosystem Modelling Research II 23-26 June 2008, Plymouth, UK.

Fulton, E., Fuller, M., Smith, A., Punt, A., 2004. Ecological indicators of the ecosystem effects of fishing: Final report. R99/1546, CSIRO Div. of Marine Research//Australian Fisheries Management Authority, CSIRO, http://dx.doi.org/10.4225/08/585c169120a95.

Grüss, A., Schirripa, M.J., Chagaris, D., Drexler, M., Simons, J., Verley, P., Shin, Y.-J., Karnauskas, M., Oliveros-Ramos, R., Ainsworth, C.H., 2015. Evaluation of the trophic structure of the West Florida shelf in the 2000s using the ecosystem model OSMOSE. J. Mar. Syst. 144, 30–47. http://dx.doi.org/10.1016/j.jmarsys.2014.11.004.

Guénette, S., Christensen, V., Pauly, D., 2008. Trophic modelling of the Peruvian upwelling ecosystem: Towards reconciliation of multiple datasets. Prog. Oceanogr. 79 (2-4), 326–335. http://dx.doi.org/10.1016/j.pocean.2008.10.005, The Northern Humboldt Current System: Ocean Dynamics, Ecosystem Processes, and Fisheries.

Gutiérrez, M., Ramirez, A., Bertrand, S., Móron, O., Bertrand, A., 2008. Ecological niches and areas of overlap of the squat lobster 'munida' *(Pleuroncodes monodon)* and anchoveta *(Engraulis ringens)* off Peru. Prog. Oceanogr. 79 (2-4), 256–263. http://dx.doi.org/10.1016/j.pocean.2008.10.019, The Northern Humboldt Current System: Ocean Dynamics, Ecosystem Processes, and Fisheries.

Gutknecht, E., Dadou, I., Le Vu, B., Cambon, G., Sudre, J., Garçon, V., Machu, E., Rixen, T., Kock, A., Flohr, A., et al., 2013. Coupled physical/biogeochemical modeling including O2-dependent processes in the eastern boundary upwelling systems: application in the benguela. Biogeosciences 10, 3559–3591. http://dx.doi.org/10.5194/bg-10-3559-2013.

Halouani, G., Lasram, F., Shin, Y.-J., Velez, L., Verley, P., Hattab, T., Oliveros-Ramos, R., Diaz, F., Ménard, F., Baklouti, M., Guyennon, A., Ms, R., Le Loc'h, F., 2016. Modelling food web structure using an end-to-end approach in the coastal ecosystem of the Gulf of Gabes (Tunisia). Ecol. Model. 339, 45–57. http://dx.doi.org/10.1016/j.ecolmodel.2016.08.008.

Hill Cruz, M., Kriest, I., José, J., Kiko, R., Hauss, H., Oschlies, A., 2021. Zooplankton mortality effects on the plankton community of the northern Humboldt Current System: sensitivity of a regional biogeochemical model. Biogeosciences 18, 2891–2916. http://dx.doi.org/10.5194/bg-18-2891-2021.

Holte, J., Talley, L.D., Gilson, J., Roemmich, D., 2017. An argo mixed layer climatology and database. Geophys. Res. Lett. 44 (11), 5618–5626. http://dx.doi.org/10.1002/2017GL073426.

Jahncke, J., Checkley, D.M., Hunt, G.L., 2004. Trends in carbon flux to seabirds in the Peruvian upwelling system: effects of wind and fisheries on population regulation. Fisheries Oceanography 13 (3), 208–223. http://dx.doi.org/10.1111/j.1365-2419.2004.00283.x.

José, Y.S., Dietze, H., Oschlies, A., 2017. Linking diverse nutrient patterns to different water masses within anticyclonic eddies in the upwelling system off Peru. Biogeosciences 14 (6), 1349–1364. http://dx.doi.org/10.5194/bg-14-1349-2017.

José, Y.S., Stramma, L., Schmidtko, S., Oschlies, A., 2019. ENSO-driven fluctuations in oxygen supply and vertical extent of oxygen-poor waters in the oxygen minimum zone of the eastern tropical south Pacific. Biogeosci. Discus. 2019, 1–20. http://dx.doi.org/10.5194/bg-2019-155.

Karstensen, J., Stramma, L., Visbeck, M., 2008. Oxygen minimum zones in the eastern tropical Atlantic and Pacific oceans. Prog. Oceanogr. 77 (4), 331–350. http://dx.doi.org/10.1016/j.pocean.2007.05.009, A New View of Water Masses After WOCE. A Special Edition for Professor Matthias Tomczak.

Kiørboe, T., 2013. Zooplankton body composition. Limnol. Oceanogr. 58 (5), 1843–1850. http://dx.doi.org/10.4319/lo.2013.58.5.1843.

López de la Lama, R., de la Puente, S., Sueiro, J.C., Chan, K.M.A., 2021. Reconnecting with the past and anticipating the future: A review of fisheries-derived cultural ecosystem services in pre-Hispanic Peru. People Nat. 3 (1), 129–147. http://dx.doi.org/10.1002/pan3.10153.

Lett, C., Verley, P., Mullon, C., Parada, C., Brochier, T., Penven, P., Blanke, B., 2008. A Lagrangian tool for modelling ichthyoplankton dynamics. Environ. Model. Softw. 23 (9), 1210–1214. http://dx.doi.org/10.1016/j.envsoft.2008.02.005.

Majluf, P., Reyes, J., 1989. The marine mammals of Peru: A review. In: Pauly, D., Muck, P., Mendo, J., Tsukayama, I. (Eds.), The Peruvian Upwelling Ecosystem: Dynamics and Interactions. ICLARM Conference Proceedings 18. Instituto del Mar del Peru (IMARPE) Callao, Peru; Deutsche Gesellschaft fuer Technische Zusammenarbeit (GIZ), GmbH, Eschbom, Federal Republic of Germany; and International Center for Living Aquatic Resources Management (ICLARM), Manila Philippines., pp. 344–363.

Marzloff, M., Shin, Y.-J., Tam, J., Travers, M., Bertrand, A., 2009. Trophic structure of the Peruvian marine ecosystem in 2000–2006: Insights on the effects of management scenarios for the hake fishery using the IBM trophic model osmose. J. Mar. Syst. 75 (1-2), 290–304. http://dx.doi.org/10.1016/j.jmarsys.2008.10.009.

Maury, O., 2010. An overview of APECOSM, a spatialized mass balanced "Apex Predators ecosystem model" to study physiologically structured tuna population dynamics in their ecosystem. Prog. Oceanogr. 84 (1-2), 113–117. http://dx.doi.org/10.1016/j.pocean.2009.09.013, Special Issue: Parameterisation of Trophic Interactions in Ecosystem Modelling.

Moriarty, R., O'Brien, T.D., 2013. Distribution of mesozooplankton biomass in the global ocean. Earth Syst. Sci. Data 5 (1), 45–55. http://dx.doi.org/10.5194/essd-5-45-2013.

Moullec, F., Barrier, N., Drira, S., Guilhaumon, F., Marsaleix, P., Somot, S., Ulses, C., Velez, L., Shin, Y.-J., 2019a. An end-to-end model reveals losers and winners in a warming Mediterranean Sea. Front. Mar. Sci. 6, 345. http://dx.doi.org/10.3389/fmars.2019.00345.

Moullec, F., Velez, L., Verley, P., Barrier, N., Ulses, C., Carbonara, P., Esteban, A., Follesa, C., Gristina, M., Jadaud, A., Ligas, A., Díaz, E.L., Maiorano, P., Peristeraki, P., Spedicato, M.T., Thasitis, I., Valls, M., Guilhaumon, F., Shin, Y.-J., 2019b. Capturing the big picture of mediterranean marine biodiversity with an end-to-end model of climate and fishing impacts. Prog. Oceanogr. 178, 102179. http://dx.doi.org/10.1016/j.pocean.2019.102179.

Muck, D.P., 1987. Monthly anchoveta consumption of guano birds, 1953 to l982. In: Pauly, D., Tsukayama, I. (Eds.), The Peruvian Anchoveta and Its Upwelling Ecosystem: Three Decades of Change. ICLARM Studies and Reviews 15. Instituto del Mar del Peru (IMARPE) Callao, Peru; Deutsche Gesellschaft fuer Technische Zusammenarbeit (GIZ), GmbH, Eschbom, Federal Republic of Germany; and International Center for Living Aquatic Resources Management (ICLARM), Manila Philippines., Instituto del Mar del Peru (IMARPE) Callao, Peru; Deutsche Gesellschaft fuer Technische Zusammenarbeit (GIZ), GmbH, Eschbom, Federal Republic of Germany; and International Center for Living Aquatic Resources Management (ICLARM), Manila Philippines., pp. 219–233.

Murphy, G., 1961. Oceanography and Variations in the Pacific Sardine Population. Technical Report, CALCOFI, pp. 55–64.

Nakai, Z., Usami, S., Hattori, S., Honjo, Y., Hayashi, S., 1955. Progress Report of the Cooperative Iwashi Resources Investigations April 1949-December 1951. Tokai Regional Fisheries Research Laboratory, p. 116.

NASA Goddard Space Flight Center, Ocean Ecology Laboratory, Ocean Biology Processing Group, 2018. Moderate-resolution imaging spectroradiometer (MODIS) Aqua chlorophyll data; 2018 reprocessing. doi:10.5067/AQUA/MODIS/L3M/CHL/2018, URL https://oceancolor.gsfc.nasa.gov/data/10.5067/AQUA/MODIS/L3M/CHL/2018/.

O'Brien, T., Moriarty, R., 2012. Global distributions of mesozooplankton abundance and biomass - gridded data product (NetCDF) - contribution to the MAREDAT world ocean atlas of plankton functional types. http://dx.doi.org/10.1594/PANGAEA.785501, PANGAEA.

Oliveros-Ramos, R., 2014. End–To–End Modelling for an Ecosystem Approach to Fisheries in the Northern Humboldt Current Ecosystem (Ph.D. thesis). University of Montpellier.

Oliveros-Ramos, R., Shin, Y.-J., 2016. Calibrar: an R package for fitting complex ecological models. arxiv, URL https://arxiv.org/abs/1603.03141.

Oliveros-Ramos, R., Verley, P., Echevin, V., Shin, Y.-J., 2017. A sequential approach to calibrate ecosystem models with multiple time series data. Prog. Oceanogr. 151, 227–244.

Paredes, C.E., Gutierrez, M.E., 2008. The Peruvian anchovy sector: Costs and benefits. An analysis of recent behavior and future challenges. In: Shriver, A.L. (Ed.), Proceedings of the Fourteenth Biennial Conference of the International Institute of Fisheries Economics & Trade, July 22-25, 2008, Nha Trang, Vietnam: Achieving a Sustainable Future: Managing Aquaculture, Fishing, Trade and Development. International Institute of Fisheries Economics & Trade, Corvallis, Oregon, USA, pp. 1–10, URL https://ir.library.oregonstate.edu/concern/conference_proceedings_or_journals/6682x476j.

Pauly, D., Vildoso, A.C., Mejia, J., Samame, M., Palomares, M.L., 1987. Population dynamics and estimated anchoveta consumption of bonito *(Sarda chiliensis)* off peru. In: Pauly, D., Tsukayama, I. (Eds.), The Peruvian Anchoveta and Its Upwelling Ecosystem: Three Decades of Change. ICLARM Studies and Reviews 15. Instituto del Mar del Peru (IMARPE) Callao, Peru; Deutsche Gesellschaft fuer Technische Zusammenarbeit (GIZ), GmbH, Eschbom, Federal Republic of Germany; and International Center for Living Aquatic Resources Management (ICLARM), Manila Philippines., pp. 325–342.

Penn, J.L., Deutsch, C., 2022. Avoiding ocean mass extinction from climate warming. Science 376 (6592), 524–526. http://dx.doi.org/10.1126/science.abe9039.

Penven, P., 2019. Croco tools. URL https://gitlab.inria.fr/croco-ocean/croco_tools/-/blob/master/Visualization_tools/.

Pikitch, E.K., Santora, C., Babcock, E.A., Bakun, A., Bonfil, R., Conover, D.O., Dayton, P., Doukakis, P., Fluharty, D., Heneman, B., Houde, E.D., Link, J., Livingston, P.A., Mangel, M., McAllister, M.K., Pope, J., Sainsbury, K.J., 2004. Ecosystem-Based Fishery Management. Science 305 (5682), 346–347. http://dx.doi.org/10.1126/science.1098222.

Pizarro, J., Docmac, F., Harrod, C., 2019. Clarifying a trophic black box: stable isotope analysis reveals unexpected dietary variation in the Peruvian anchovy *Engraulis ringens*. PeerJ 7, e6968. http://dx.doi.org/10.7717/peerj.6968.

PRODUCE, 2013. Anuario estadístico pesquero y acuicola 2012. Ministerio de la Producción - PRODUCE, Lima, Peru, URL https://sinia.minam.gob.pe/documentos/anuario-estadistico-pesquero-acuicola-2012.

Ridgway, K., Dunn, J., Wilkin, J., 2002. Ocean interpolation by four-dimensional weighted least squares—Application to the waters around Australasia. J. Atmos. Ocean. Technol. 19 (9), 1357–1375. http://dx.doi.org/10.1175/1520-0426(2002)019<1357:OIBFDW>2.0.CO;2.

Rose, K.A., Fiechter, J., Curchitser, E.N., Hedstrom, K., Bernal, M., Creekmore, S., Haynie, A., ichi Ito, S., Lluch-Cota, S., Megrey, B.A., Edwards, C.A., Checkley, D., Koslow, T., McClatchie, S., Werner, F., MacCall, A., Agostini, V., 2015. Demonstration of a fully-coupled end-to-end model for small pelagic fish using sardine and anchovy in the California Current. Prog. Oceanogr. 138, 348–380. http://dx.doi.org/10.1016/j.pocean.2015.01.012, Combining Modeling and Observations to Better Understand Marine Ecosystem Dynamics.

Roy, C., 1993. The optimal environmental window hypothesis: A non linear environmental process affecting recruitment success. ICES J. Mar. Sci. 76, 1–13.

Schwartzlose, R.A., Alheit, J., Bakun, A., Baumgartner, T.R., Cloete, R., Crawford, R.J.M., Fletcher, W.J., Green-Ruiz, Y., Hagen, E., Kawasaki, T., Lluch-Belda, D., Lluch-Cota, S.E., MacCall, A.D., Matsuura, Y., Nevárez-Martínez, M.O., Parrish, R.H., Roy, C., Serra, R., Shust, K.V., Ward, M.N., Zuzunaga, J.Z., 1999. Worldwide large-scale fluctuations of sardine and anchovy populations. South Afr. J. Mar. Sci. 21 (1), 289–347. http://dx.doi.org/10.2989/025776199784125962.

Shchepetkin, A.F., McWilliams, J.C., 2005. The regional oceanic modeling system (ROMS): a split-explicit, free-surface, topography-following-coordinate oceanic model. Ocean Model. 9 (4), 347–404. http://dx.doi.org/10.1016/j.ocemod.2004.08.002.

Shin, Y.-J., Cury, P., 2001. Exploring fish community dynamics through size-dependent trophic interactions using a spatialized individual-based model. Aquat. Living Resour. 14 (2), 65–80. http://dx.doi.org/10.1016/S0990-7440(01)01106-8.

Shin, Y.-J., Cury, P., 2004. Using an individual-based model of fish assemblages to study the response of size spectra to changes in fishing. Can. J. Fish. Aquat. Sci. 61 (3), 414–431. http://dx.doi.org/10.1139/f03-154.

Tam, J., Taylor, M.H., Blaskovic, V., Espinoza, P., Michael Ballón, R., Díaz, E., Wosnitza-Mendo, C., Argüelles, J., Purca, S., Ayón, P., Quipuzcoa, L., Gutiérrez, D., Goya, E., Ochoa, N., Wolff, M., 2008. Trophic modeling of the northern Humboldt current ecosystem, part I: Comparing trophic linkages under La Niña and El Niño conditions. Prog. Oceanogr. 79 (2-4), 352–365. http://dx.doi.org/10.1016/j.pocean.2008.10.007, The Northern Humboldt Current System: Ocean Dynamics, Ecosystem Processes, and Fisheries.

Taylor, M.H., Tam, J., Blaskovic, V., Espinoza, P., Michael Ballón, R., Wosnitza-Mendo, C., Argüelles, J., Díaz, E., Purca, S., Ochoa, N., Ayón, P., Goya, E., Gutiérrez, D., Quipuzcoa, L., Wolff, M., 2008. Trophic modeling of the Northern Humboldt current ecosystem, Part II: Elucidating ecosystem dynamics from 1995 to 2004 with a focus on the impact of ENSO. Prog. Oceanogr. 79 (2-4), 366–378. http://dx.doi.org/10.1016/j.pocean.2008.10.008, The Northern Humboldt Current System: Ocean Dynamics, Ecosystem Processes, and Fisheries.

Tittensor, D.P., Eddy, T.D., Lotze, H.K., Galbraith, E.D., Cheung, W., Barange, M., Blanchard, J.L., Bopp, L., Bryndum-Buchholz, A., Büchner, M., Bulman, C., Carozza, D., Christensen, V., Coll, M., Dunne, J., Fernandes, J., Fulton, E., Hobday, A., Huber, V., Jennings, S., Jones, M., Lehodey, P., Link, J., Mackinson, S., Maury, O., Niiranen, S., Oliveros-Ramos, R., Roy, T., Schewe, J., Shin, Y.-J., Silva, T., Stock, C., Steenbeek, J., Underwood, P., Volkholz, J., Watson, J., Walker, N., 2018. A protocol for the intercomparison of marine fishery and ecosystem models: Fish-MIP v1. 0. Geosci. Model Dev. 11 (4), 1421–1442. http://dx.doi.org/10.5194/gmd-11-1421-2018.

Travers, M., 2009. Couplage De Modèles Trophiques Et Effets Combinés De La Pêche Et Du Climat, Coupling Trophodynamic Models for Assessing the Combined Effects of Fishing and Climate (Ph.D. thesis). Université Pierre et Marie Curie, URL https://archimer.ifremer.fr/doc/00003/11445/.

Travers, M., Shin, Y.-J., Jennings, S., Machu, E., Huggett, J., Field, J., Cury, P., 2009. Two-way coupling versus one-way forcing of plankton and fish models to predict ecosystem changes in the benguela. Ecol. Model. 220 (21), 3089–3099. http://dx.doi.org/10.1016/j.ecolmodel.2009.08.016, Selected Papers from the Sixth European Conference on Ecological Modelling - ECEM '07, on Challenges for ecological modelling in a changing world: Global Changes, Sustainability and Ecosystem Based Management, November 27-30, 2007, Trieste, Italy.

Travers, M., Shin, Y.-J., Shannon, L., Cury, P., 2006. Simulating and testing the sensitivity of ecosystem-based indicators to fishing in the southern Benguela ecosystem. Can. J. Fish. Aquat. Sci. 63 (4), 943–956. http://dx.doi.org/10.1139/f06-003.

Travers-Trolet, M., Shin, Y., Field, J., 2014a. An end-to-end coupled model ROMS-n2p2z2d2-OSMOSE of the southern benguela foodweb: parameterisation, calibration and pattern-oriented validation. Afr. J. Mar. Sci. 36 (1), 11–29. http://dx.doi.org/10.2989/1814232X.2014.883326.

Travers-Trolet, M., Shin, Y.-J., Shannon, L.J., Moloney, C.L., Field, J.G., 2014b. Combined fishing and climate forcing in the southern benguela upwelling ecosystem: an end-to-end modelling approach reveals dampened effects. PLoS One 9 (4), e94286. http://dx.doi.org/10.1371/journal.pone.0094286.

Tsikliras, A.C., Froese, R., 2019. Maximum sustainable yield. In: Fath, B.D. (Ed.), Encyclopedia of Ecology, Vol. 1, second ed. Elsevier, pp. 108–115. http://dx.doi.org/10.1016/B978-0-12-409548-9.10601-3.

Vergnon, R., Shin, Y.-J., Cury, P., 2008. Cultivation, Allee effect and resilience of large demersal fish populations. Aquat. Living Resour. 21 (3), 287–295. http://dx.doi.org/10.1051/alr:2008042.

Ware, D., 1992. Production characteristics of upwelling systems and the trophodynamic role of hake. South Afr. J. Mar. Sci. 12 (1), 501–513. http://dx.doi.org/10.2989/02577619209504721.

Watson, J.R., Stock, C.A., Sarmiento, J.L., 2015. Exploring the role of movement in determining the global distribution of marine biomass using a coupled hydrodynamic – size-based ecosystem model. Prog. Oceanogr. 138, 521–532. http://dx.doi.org/10.1016/j.pocean.2014.09.001, Combining Modeling and Observations to Better Understand Marine Ecosystem Dynamics.

Xing, L., Chongliang, Z., Chen, Y., Shin, Y.-J., Verley, P., Yu, H., Ren, Y., 2017. An individual-based model for simulating the ecosystem dynamics of Jiaozhou Bay, China. Ecol. Model. 360, 120–131. http://dx.doi.org/10.1016/j.ecolmodel.2017.06.010.

Xue, T., Frenger, I., Prowe, A., José, Y.S., Oschlies, A., 2022. Mixed layer depth dominates over upwelling in regulating the seasonality of ecosystem functioning in the Peruvian upwelling system. Biogeosciences 19 (2), 455–475. http://dx.doi.org/10.5194/bg-19-455-2022.